



PII S0016-7037(99)00005-8

## Oxygen isotope fractionation in ferric oxide-water systems: Low temperature synthesis

HUIMING BAO<sup>\*,†</sup> and PAUL L. KOCH<sup>‡</sup>

Department of Geosciences, Princeton University, Princeton, NJ 08544, USA

(Received September 16, 1998; accepted January 18, 1999)

**Abstract**—The magnitude and temperature-sensitivity of oxygen isotope fractionation in ferric oxide-water systems remain uncertain. In this study, three different synthetic methods are used to investigate the temperature dependence of the fractionation between water and hematite, akaganeite, and goethite at near-surface temperatures. Our results reveal two similarities among these ferric oxide-water systems. First, the fractionation of oxygen isotopes between water and ferric oxide is small (i.e., ferric oxide-water fractionation factors [ $\alpha$ ] are very close to 1.000). Second, these  $\alpha$  values are relatively insensitive to change in temperature ( $T$ ). Hematite-water has a slightly higher  $\alpha$  value and a greater temperature sensitivity than goethite-water at surface temperatures. While the issue requires further study, we speculate that differences in the washing and drying protocols applied to final precipitates may be one of the factors that have contributed to the discrepancies among published  $\alpha$ - $T$  curves.

Owing to the rapid exchange of oxygen among the various hydrolytic Fe(III) species and ambient water, oxygen isotope equilibrium is probably attained between water and the ferric oxide gels and poorly-ordered ferrihydrite that are the initial precipitates in nearly all natural settings. Aging experiments suggest that isotopic compositions carried by ferric oxide gels and ferrihydrite are almost entirely erased by later exchange with ambient water during the maturation processes leading to formation of either hematite or goethite. These results suggest that dissolution and reprecipitation occur in the supposedly “solid-state transformation” from ferrihydrite to hematite. Thus the  $\delta^{18}\text{O}$  value of natural crystalline ferric oxides may provide a record of the long-term average  $\delta^{18}\text{O}$  value of local surface water, rather than that of the water from which the solid ferric oxide first formed. Copyright © 1999 Elsevier Science Ltd

### 1. INTRODUCTION

Ferric oxides (a term used here to include oxides and oxyhydroxides phases) are abundant in a variety of geologic settings. Hematite ( $\alpha\text{-Fe}_2\text{O}_3$ ) and goethite ( $\alpha\text{-FeOOH}$ ) are the two most common stable ferric oxide phases. Many ferric oxides occur as authigenic minerals in sedimentary deposits, such as banded iron formations (James and Trendall, 1982), oolitic ironstones (Petránek and Van Houten, 1997), iron-cemented sandstones (Walker et al., 1981; Lu et al., 1994), and iron-enriched soil horizons (Van Houten, 1973; Nahon, 1986; Cornell and Schwertmann, 1997).

The oxygen isotope composition of ferric oxides has been used to monitor ancient surface environments (Yapp, 1987, 1990b, 1993a, 1993b; Bird et al., 1992; Bao et al., in press). The fractionation of oxygen isotopes between a mineral and a fluid can be fit by an equation of the form:

$$1000\ln\alpha = A \times 10^6/T^2 + B \quad (1)$$

where  $\alpha$  is the fractionation factor (defined as  $^{18}\text{O}/^{18}\text{O}_{\text{mineral}}/^{18}\text{O}/^{18}\text{O}_{\text{fluid}}$ ).  $T$  is the temperature of mineral formation in kelvin, and  $A$  and  $B$  are constants. For OH-bearing minerals at near surface temperatures,  $10^3/T$  is often used rather than  $10^6/T^2$  (Clayton and Epstein, 1961). Thus the oxygen isotope

composition ( $\delta^{18}\text{O}$ ) of a mineral is determined by the formation temperature and the  $\delta^{18}\text{O}$  of the formation water.

While prior isotopic results obtained for ferric oxides are promising, the systematics of oxygen isotope fractionation in this system remain controversial. Low-temperature synthesis experiments (Yapp, 1990a; Müller, 1995), extrapolation from coexisting hydrothermal minerals (Clayton and Epstein, 1961), and semi-theoretical calculations (Zheng, 1991, 1998) all produce different  $\alpha$ - $T$  relations. Application of different  $\alpha$ - $T$  curves results in radically different interpretations of formation conditions for natural ferric oxides (Bao et al., in press). A well-defined fractionation relation is crucial if oxygen isotope compositions of ferric oxides are to provide reliable and quantitative information for paleoclimatic and paleohydrological research. Here we report our study of oxygen isotope systematics in ferric oxide-water systems conducted through a series of synthesis and exchange (aging) experiments, compare with previous calibrations, and discuss the geological implications of our results.

#### 1.1. Results of Prior Synthesis Experiments

Yapp (1987, 1990a) conducted synthesis experiments to determine the  $\alpha$ - $T$  relation in the goethite (hematite)-water system, in which goethite and/or hematite were synthesized at temperatures ranging from 25°C to 120°C. He concluded that the oxygen isotope fractionation factors for these two ferric oxides are identical, with a relation to temperature of

$$1000\ln\alpha = 1.63 \times 10^6/T^2 - 12.3 \quad (2)$$

Recent studies of ancient and modern goethite samples appear

\*Author to whom correspondence should be addressed.

†Present address: Department of Chemistry & Biochemistry, Mail Code 0356, University of California, San Diego, La Jolla, CA 92093, USA.

‡Present address: Department of Earth Sciences, E&MS Bldg., University of California, Santa Cruz, CA 95064, USA.

Table 1. Methods used in synthesis and exchange experiments.

| Method                                    | Description <sup>a</sup>  |
|---|---|
| Forced-Hydrolysis                         | Add 2.7 g FeCl <sub>3</sub> · 6H <sub>2</sub> O to 500 mL 0.002 M HCl at designated temperature, stir vigorously. Temperature: 35°, 50°, 70°, 95°, 115°, and 140°C.   |
| NaOH                                      | Add 3.38 g FeCl <sub>3</sub> · 6H <sub>2</sub> O to 12.5 mL water. Once dissolved, add 22.5 mL 5 M NaOH. Stir and shake vigorously, then dilute to 250 mL. OH/Fe ratio ≈ 9. Temperature: 35°, 50°, 70°, 95°, 115°, and 140°C.   |
| NaOH + HCO <sub>3</sub> <sup>-</sup>      | Add 6.69 g FeCl <sub>3</sub> · 6H <sub>2</sub> O to 125 mL water. Once dissolved, add 75 mL 1 M NaOH. Stir vigorously, then add 17 mL 1 M NaHCO <sub>3</sub> . OH/Fe ratio ≈ 3, and HCO <sub>3</sub> <sup>-</sup> /Fe ratio ≈ 0.7. Temperature: 30°, 37°, 50°, 70°, 95°, 115°, and 140°C. |
| Fh-exchange                               | Add 18 g FeCl <sub>3</sub> · 6H <sub>2</sub> O to 500 mL water (δ <sup>18</sup> O = -8.0‰). Once dissolved, add 330 mL 1 M NaOH (solution made with -8.0‰ water), stir vigorously. After 10–15 minutes, obtain ferrihydrite gel by centrifugation. Place aliquots of gel in:              |
| OH + HCO <sub>3</sub> <sup>-</sup> method | 1) 62.5 mL water + 37.5 mL 1 M NaOH + 8.5 mL 1 M NaHCO <sub>3</sub> , where water and solutions had three different δ <sup>18</sup> O values (+1.8‰, -8.0‰, and -15.1‰). Temperature: 75°C.   |
| HCO <sub>3</sub> <sup>-</sup> method      | 2) 95 mL water + 13.5 mL 1 M NaHCO <sub>3</sub> , where water and solutions had three different δ <sup>18</sup> O values (+1.8‰, -8.0‰, and -15.1‰). Temperature: 30° and 75°C.   |

<sup>a</sup>Quantity of chemicals were proportionally reduced in higher temperature aging experiments which required use of a bomb.

to support this finding (Yapp, 1993b, 1997; Girard et al., 1997). Data obtained from high pH solutions (OH/Fe = 12.5) were off the relations and were excluded because kinetic isotope effect was suspected in these fast precipitating experiments (Yapp, 1987).

Müller (1995) obtained three different  $\alpha$ - $T$  relations for ferric oxide-water systems from three different methods of synthesis:

$$\text{KOH-method: } 1000\ln\alpha = 1.1 \times 10^6/T^2 - 12.1 \quad (3a)$$

$$\text{NaOH-method: } 1000\ln\alpha = 0.3 \times 10^6/T^2 - 3.0 \quad (3b)$$

$$\text{Hydrolysis: } 1000\ln\alpha = 2.76 \times 10^6/T^2 - 23.7 \quad (3c)$$

The results from the two base-added methods were similar at lower temperatures, especially when compared with the results from the hydrolysis method, which produced an  $\alpha$  value that was relatively sensitive to temperature. Müller's (1995) study of Tertiary lateritic samples from Central Nigeria suggests that the fractionation relations derived from his base-added methods best fit the formation conditions of natural goethite or mixtures of goethite and hematite.

## 1.2. Approach of This Study

A re-examination of low-temperature oxygen isotope fractionation in ferric oxide-water systems is warranted for three reasons. First, recently we have been examining naturally occurring pedogenic hematites from the Paleogene of Wyoming and ferric oxides from Holocene and Pleistocene soils and groundwater systems to address paleoclimatic and paleohydrologic questions (Bao, 1998; Bao et al., in press). We have found it difficult to reconcile data from natural systems with the widely used Eqn. 2 under plausible sets of formation conditions.

Second, as noted above, the  $\alpha$ - $T$  curves obtained in synthesis experiments by different workers are quite different (e.g., Yapp, 1990a; Müller, 1995). The cause of these large discrepancies is unclear. Many of these prior experiments were not designed to yield pure ferric oxide phases, however, and in some experiments, chemical conditions were not the same at different temperatures (e.g., a base-added method might be

used at lower temperatures, whereas forced-hydrolysis was used at higher temperatures). Consequently, prior synthesis results have left two questions unresolved. If chemical conditions are controlled so that only one ferric oxide phase is produced, will different phases (e.g., hematite, goethite, and akaganeite [ $\beta$ -FeOOH]) follow different  $\alpha$ - $T$  relations? Alternatively, if the same phase is formed under different chemical conditions or by different pathways, will it follow the same  $\alpha$ - $T$  relation?

Finally, in nature, metastable phases such as ferrihydrite (Fh) and poorly-crystalline, ferric gels are often the kinetically-favored initial precipitates. It typically takes centuries to tens of thousands of years for these metastable phases to transform into highly-crystalline ferric oxide, depending on physiochemical conditions. The behavior of oxygen isotopes during transformation is unclear. The currently accepted mechanism for goethite formation from Fh is via dissolution-reprecipitation, whereas hematite formation from Fh is thought to involve internal rearrangement or solid-state transformation, without dissolution-reprecipitation. Therefore in goethite, the oxygen isotope composition of the initial Fh may be lost and the ultimate isotopic signal would reflect exchange with pore fluids during aging. As a result of the solid-state transformation hypothesized for hematite formation, the  $\delta^{18}\text{O}$  of this phase may be related solely to the  $\delta^{18}\text{O}$  of the original fluid from which precursor Fh formed. Answers to these questions are of critical importance to the interpretation of  $\delta^{18}\text{O}$  of natural ferric oxides.

We explore the first two issues regarding the  $\alpha$ - $T$  relation with three experiments (Table 1): synthesis of ferric oxide by forced hydrolysis of acidic Fe(III) solutions at six temperatures ranging from 35°C to 140°C (forced-hydrolysis experiment); synthesis of ferric oxide by transformation of Fh in a strongly-alkaline medium at the same six temperatures (NaOH experiment); and synthesis of ferric oxide by transformation of Fh over approximately the same range of temperatures in an alkaline solution buffered by addition of HCO<sub>3</sub><sup>-</sup> (NaOH + HCO<sub>3</sub><sup>-</sup> experiment). The forced-hydrolysis experiments are expected to generate akaganeite at lower temperatures and hematite at higher temperatures. The NaOH experiments should generate pure goethite at low to moderate temperatures. NaOH + HCO<sub>3</sub><sup>-</sup>

experiments should generate pure hematite across this range of temperatures. If hematites from the forced-hydrolysis experiments and from the NaOH + HCO<sub>3</sub><sup>-</sup> experiments exhibit no significant differences in the  $\alpha$ -*T* relation, we may conclude that different formation conditions and/or pathways have little effect on isotopic fractionation in the hematite-water system. The effects of differing mineralogy on fractionation will be revealed by comparing  $\alpha$ -*T* relations for pure hematite (NaOH + HCO<sub>3</sub><sup>-</sup> experiment) to pure goethite (NaOH experiment), and pure akaganeite (forced-hydrolysis experiment). We will also examine the effect of initial Fe(III) concentration (0.2 M or 0.02 M) on the  $\delta^{18}\text{O}$  of the final hematite precipitate in forced-hydrolysis solutions at three different temperatures.

To examine the potential for isotopic inheritance from initial precipitates, we synthesized a kinetically metastable phase: 2-line Fh, from a solution with a unique  $\delta^{18}\text{O}$  value, then aged the Fh to either hematite or goethite in solutions with three different  $\delta^{18}\text{O}$  values (Table 1, Fh-exchange experiment). If the final precipitate has a  $\delta^{18}\text{O}$  value that indicates complete equilibration with the aging solutions, rather than the initial solution from which Fh precipitated, we may conclude that the Fh-to-goethite and Fh-to-hematite transformations are isotopically open processes. If not, the extent of exchange can be estimated from the isotopic data. These simple experiments will shed new light on the mechanisms of Fh-to-goethite and Fh-to-hematite transformation.

## 2. METHODS

In most natural aquatic systems, Fe(III) precipitation occurs very slowly by the oxygenation of Fe(II) and subsequent hydrolysis. We opted for direct Fe(III) hydrolysis to obtain crystalline ferric oxides for all our experiments because this method can be easily manipulated to produce pure mineral phases. Fe(III) hydrolysis has been studied intensively, and there is a voluminous literature on the formation and characteristics of hydrolytic Fe(III) and polymer species, the pattern and kinetics of nucleation, the processes by which amorphous Fe(III) hydroxide hydrates age to more crystalline products, the effect of OH/Fe ratio and other ions on the crystallinity of precipitates, and the kinetics of phase transformation (see reviews by Flynn, 1984; Schneider and Schwyn, 1987; Cornell et al., 1989). Therefore, considering that our focus is oxygen isotope fractionation, we did not monitor precise changes in pH and [Fe<sup>3+</sup>] during the course of sample aging or evaluate the crystal forms of final precipitates. However, solution pH was measured at the start and end of sample aging.

Hematite, goethite, and akaganeite were prepared by three different experiments, as outlined in Table 1, generally following techniques described by Schwertmann and Cornell (1991). Fe(III) salt (FeCl<sub>3</sub> · 6H<sub>2</sub>O, lumps, analytical reagent grade, Thomas Scientific) was used in all experiments. Other Fe(III) sources, such as Fe(NO<sub>3</sub>)<sub>3</sub> · 9H<sub>2</sub>O and Fe(ClO<sub>4</sub>)<sub>3</sub>, which have been used in similar synthesis experiment, were not chosen, because we were attempting to (1) obtain akaganeite, which requires the presence of Cl<sup>-</sup> in solution and (2) avoid the excessive sample washing required to thoroughly clean residual NO<sub>3</sub><sup>-</sup> and ClO<sub>4</sub><sup>-</sup> from precipitates before isotopic analysis. Doubly deionized (DD) water with a  $\delta^{18}\text{O}$  value of  $-8.0 \pm 0.1\text{‰}$  was used in all synthesis experiments. Polyethylene bottles were used for experiments at temperatures  $\leq 95^\circ\text{C}$ ; acid digestion bombs (45 mL, Parr Instrument Company) were used for experiments at temperatures  $>100^\circ\text{C}$ . All solutions were preheated to the designated temperature before reactant solutions were mixed, except for experiments at  $115^\circ\text{C}$  and  $140^\circ\text{C}$  where solutions were mixed at  $95^\circ\text{C}$  and then quickly brought to designated temperatures. Every experiment was conducted in duplicate.

For the Fh-exchange experiments, we obtained Fh by adding 1 M NaOH to a FeCl<sub>3</sub> solution with a final OH/Fe ratio of  $\sim 3.8$  (method of Schwertmann and Cornell, 1991). These initial solutions were made with DD water, thus this Fh gel should have initially equilibrated with

this  $-8.0\text{‰}$  water. Dark-red Fh gel was collected by centrifugation after the solution was aged at the designated temperature for 10–20 min. Aliquots of gel were then added to solutions with three different  $\delta^{18}\text{O}$  values ( $+1.8\text{‰}$ ,  $-8.0\text{‰}$ ,  $-15.1\text{‰}$ ) for aging to final crystalline precipitates. Vigorous shaking of aging solutions at the start is especially important, because Fh gels tend to form aggregates that are difficult to disperse. This experiment was performed at two temperatures,  $75^\circ\text{C}$  and  $30^\circ\text{C}$ . Two different aging solutions (NaOH + HCO<sub>3</sub><sup>-</sup> and HCO<sub>3</sub><sup>-</sup>) were used in the  $75^\circ\text{C}$  experiments to obtain both hematite and goethite (Table 1). All solutions (e.g., NaOH, NaHCO<sub>3</sub>) were made using water with the same  $\delta^{18}\text{O}$  value as that of the water added to the aging solution. The contribution of oxygen to these solutions from NaOH and NaHCO<sub>3</sub> was insignificant. During all of our experiments, bottles and bombs were sealed at all times, except for the initial short period when different solutions were mixed. Solution levels were at least  $>2/3$  of the maximum volume of the bottles.  $\delta^{18}\text{O}$  values of initial or final solutions were measured to ensure that the target isotopic composition of the aging solution had been reached, and that no shifts occurred during the course of the experiments. Every Fh-exchange experiment was also conducted in duplicate.

For both synthesis and Fh-exchange experiments, precipitates were collected by centrifugation, then washed twice with DD water. Each precipitate (except for those from forced-hydrolysis experiments) was treated with  $\sim 0.5$  M HCl for  $\sim 30$  min to dissolve residual Fh or other poorly-crystalline and amorphous phases, then rinsed again with DD water and centrifuged. Several drops of saturated NaBr solution were sometimes added to the centrifuge tube to promote coagulation of fine particles to reduce centrifugation times. We did not measure the HCO<sub>3</sub><sup>-</sup> concentration in the precipitates obtained from experiments involving buffered solutions, but believe that it should be minimal after washing and soaking with HCl. The precipitates were then dried under vacuum, mostly in a freeze drier but a few were vacuum-dried at room temperature.

We believe that acid washing and vacuum-drying are crucial steps for obtaining reliable  $\delta^{18}\text{O}$  values from these fine-grained, low-temperature precipitates, due to the presence of significant concentrations of amorphous phases in final precipitates. Amorphous phases contain large amount of water, and if not leached from precipitates prior to oven drying, these amorphous phases may transform into crystalline phases and record isotopic signals from evaporating water. The content of amorphous ferric oxide phases in final precipitates from various experiments was determined by measuring the amount of oxalate-extractable from oxides in final precipitates. Final precipitates were neutralized with HCl and washed clean with DD water before freeze-drying for two days. Immediately after being removed from the freeze-dryer, the precipitates were weighed and subsequently treated with 0.2 M ammonium oxalate-oxalic acid (pH = 3) in the dark for 2 hr. This is a standard procedure for extracting non-crystalline ferric oxides from soils or to leach poorly-crystalline phases from precipitates in synthesis experiments (McKeague and Day, 1966; Schwertmann and Cornell, 1991). [Fe] and [Na] were determined by atomic absorption spectrometer (AA) at University of California Santa Cruz.

We also collected an aliquot of precipitate from one  $30^\circ\text{C}$  NaOH + HCO<sub>3</sub><sup>-</sup> experiment. The precipitate was washed with DD water twice and oven-dried at  $100^\circ\text{C}$  without HCl treatment (sample CH-20A\*) in order to compare the effect of drying procedures on the final  $\delta^{18}\text{O}$  of the precipitate. Similarly a 2-line Fh sample from a Fh-exchange experiment was dried at  $50^\circ\text{C}$  for three days and subsequently analyzed by X-ray diffraction.

X-ray diffraction (XRD) patterns were obtained from most precipitates, using a Scintag PAD-V  $\theta$ - $2\theta$  diffractometer with a Cu K $\alpha$  radiation source at a scan rate of  $2^\circ$   $2\theta/\text{min}$  at the Department of Geosciences, Princeton University.

The  $\delta^{18}\text{O}$  values of solutions were determined by CO<sub>2</sub> equilibration using a Micromass Isoprep 18 automated water analysis system interfaced with an Optima isotope-ratio monitoring mass spectrometer in the Department of Geosciences, Princeton University. One or two beads of NaOH were added to strongly acidic solutions and several drops of H<sub>3</sub>PO<sub>4</sub> were added to strongly alkaline solutions to neutralize the solutions prior to loading into glass vessels for CO<sub>2</sub> equilibration. The amount of added H<sub>3</sub>PO<sub>4</sub> is small and H<sub>3</sub>PO<sub>4</sub> is inert to oxygen exchange with water samples during our experiment time scale and pH/temperature conditions (Tudge, 1960; Gamsjäger and Murmann,

1983). The oxygen from the added NaOH beads is also minimal compared to that in the whole water sample. Approximately 5 mL of fluid was equilibrated at 25°C with CO<sub>2</sub> gas overnight. The CO<sub>2</sub> was dried cryogenically, then transferred to the mass spectrometer. The standard deviation for replicate analyses of a standard laboratory H<sub>2</sub>O was  $\pm 0.1\%$ .

The  $\delta^{18}\text{O}$  value of ferric oxides was measured by CO<sub>2</sub> laser fluorination at the Geophysical Laboratory, Carnegie Institution, Washington, DC. Powdered samples (~2 mg) were loaded into a stainless steel holder along with a reference sample. Samples were prefluorinated overnight at room temperature prior to O<sub>2</sub> extraction. The color of most hematites precipitated below 70°C in NaOH + HCO<sub>3</sub><sup>-</sup> experiments and a few akaganeite samples precipitated below 70°C in forced-hydrolysis experiments changed from red or reddish-brown to dark-brown during prefluorination. XRD analysis of the prefluorinated dark-brown powders revealed no change in mineralogy. Oxygen yields were near 100%, indicating minimal loss of structural oxygen during color change. Most ferric oxide powders were “well-behaved” and did not sputter excessively during laser heating. Samples with more NaBr sputtered more, thus addition of NaBr during centrifugation should be kept to a minimum. O<sub>2</sub> was collected in a sample vessel containing molecular sieve at -196°C and analyzed on a Finnegan MAT 252 mass spectrometer. The mean difference in  $\delta^{18}\text{O}$  between duplicate analyses was <0.3%.

Oxygen isotope compositions of water and ferric oxide are expressed as:

$$\delta^{18}\text{O} = (R_{\text{sample}} - R_{\text{standard}}) \times 1000/R_{\text{standard}} \quad (4)$$

where  $R_{\text{sample}}$  and  $R_{\text{standard}}$  refer to the ratio of <sup>18</sup>O to <sup>16</sup>O in the sample and standard, respectively. All results are given relative to the SMOW international reference standard.

### 3. RESULTS

#### 3.1. Mineral Phase of Precipitates

Experimental results are given in Table 2. Pure goethite was obtained at all temperatures in the NaOH experiments, except at 140°C, where the sample contained a minor amount of hematite. Pure hematite was obtained from all NaOH + HCO<sub>3</sub><sup>-</sup> experiments, except for several low-temperature ( $\leq 37^\circ\text{C}$ ) syntheses that yielded trace amounts of goethite. Pure hematite was also produced by forced-hydrolysis experiments at 115°C and 140°C. Pure akaganeite was formed in forced-hydrolysis experiments at temperatures  $\leq 70^\circ\text{C}$ . Interestingly, forced-hydrolysis experiments at 95°C produced pure hematite when the initial [Fe<sup>3+</sup>] was 0.02 M, but a mixture of akaganeite and hematite formed when the initial [Fe<sup>3+</sup>] was 0.2 M. We also observed that during the course of the forced-hydrolysis experiments at 95° and 115°C, purple-red hematite formed by transformation from an earlier yellow precipitate, presumably goethite. However, hematite precipitated directly from purple-red Fh (without a yellow intermediate) in the NaOH + HCO<sub>3</sub><sup>-</sup> experiments at all temperatures.

During the Fh-exchange experiments, final precipitates were pure goethite in the NaOH + HCO<sub>3</sub><sup>-</sup> solution, and pure hematite in the HCO<sub>3</sub><sup>-</sup> solution. Initial air-dried Fh gel exhibited no conspicuous diffraction peaks. However, after oven-drying at 50°C for 3 days, XRD patterns showed clear peaks of both hematite and goethite.

#### 3.2. Yield and Crystallinity

Synthesis yield is calculated as ratio of the weight of ferric oxide precipitate over the predicted weight of ferric oxide assuming all added Fe salt in solution precipitated out as ferric oxide. The NaOH experiments generally had nearly 100% yields. The NaOH + HCO<sub>3</sub><sup>-</sup> experiments had yields that in-

creased with temperature from >88% at lower temperatures to nearly 100% at temperatures  $\geq 95^\circ\text{C}$ . The forced-hydrolysis experiments had much lower yields when compared with the other two methods, especially at lower temperatures, but 80% to 100% yields were obtained at 115°C and 140°C. An interesting feature of the forced-hydrolysis experiments is that, at 115°C and 140°C, experiments with initial [Fe<sup>3+</sup>] of 0.2 M had only 1/2 to 2/3 the yield of the experiments with initial [Fe<sup>3+</sup>] of 0.02 M, although they all produced pure hematite.

The crystallinity of a precipitate refers to particle size as well as the degree of lattice strain and defects. The crystallinity of precipitates differs among the experiments. A semi-quantitative estimate of particle size can be derived from height/width ratio of the major XRD peak, if differences in lattice strain and defect are considered unimportant. In general, higher synthesis temperatures generated precipitates of higher crystallinity. Precipitates obtained from forced-hydrolysis experiments had broader peaks (indicating poorer crystallinity) than those from NaOH or NaOH + HCO<sub>3</sub><sup>-</sup> experiments. Hematite produced by forced-hydrolysis at higher temperatures ( $\geq 95^\circ\text{C}$ ) from solutions with initial [Fe<sup>3+</sup>] of 0.2 M had poorer crystallinity than those from solutions with initial [Fe<sup>3+</sup>] of 0.02 M. Interestingly, HCl-washed and vacuum-dried sample CH-20A exhibited higher crystallinity than its non-HCl-washed, oven-dried equivalent (CH-20A\*) (Table 2).

#### 3.3. Content of Oxalate-Extractable Ferric Oxides in Precipitates

Amorphous ferric oxides such as Fh are often the kinetically stable phases during the precipitation of ferric oxides from Fe<sup>3+</sup>. Therefore, the content of amorphous phases in a precipitate is determined by a number of variables (e.g., initial [Fe<sup>3+</sup>], solution OH:Fe ratio, temperature, and duration) that affect reaction kinetics. We tested selected experimental conditions to see if the content of amorphous phases varies with these variables. As shown in Table 3, temperature has the most obvious impact on amorphous content, with the low temperature synthesis (e.g., 30°C) sometimes producing more than half amorphous phases in the precipitates. Higher initial [Fe<sup>3+</sup>], lower OH:Fe ratio, or short duration tend to yield significantly more amorphous phase in precipitates than otherwise. It should be emphasized that the reported contents of amorphous phases should be considered as minimum values, because washing and freeze-drying prior to analysis by AA may reduce the amount of oxalate-extractable ferric oxides.

#### 3.4. Oxygen Isotope Composition of Formation Solutions

The same initial DD water ( $\delta^{18}\text{O} = -8.0 \pm 0.1\%$ ) was used for synthesis experiments. We measured the  $\delta^{18}\text{O}$  of final solutions for every experiment, and only two experiments had to be discarded and repeated due to leakage in polyethylene bottles (as revealed by higher  $\delta^{18}\text{O}$  values for final solutions). There was no difference in  $\delta^{18}\text{O}$  between the initial and final solutions for the data reported here. The small amounts of NaOH and NaHCO<sub>3</sub> used in the experiments had no effect on the  $\delta^{18}\text{O}$  of the solution as a whole. This is expected from the large ratio of water to precipitate in the experiments. The oxygen contributed from NaOH is <1% of the total oxygen in

Table 2. Chemical conditions and mineralogical data for three synthesis experiments.

| Sample  | <i>t</i><br>(°C) | Duration | Solution pH<br>initial | Solution pH<br>final | Initial [Fe]<br>(M) | HCl<br>washing | XRD result <sup>a</sup><br>Mineralogy | FWHM <sup>b</sup><br>(°2θ) | % Yield |
|---|------------------|----------|------------------------|----------------------|---------------------|----------------|---------------------------------------|----------------------------|---------|
| Hydrolysis experiment (OH/Fe = 0)                           |                  |          |                        |                      |                     |                |                                       |                            |         |
| CH-12A  | 140              | 24 hr    | 3.5–4.0                | 0.0–0.5              | 0.200               | no             | Hmt                                   | 0.30                       | 62%     |
| CH-12B  | 140              | 24 hr    | 3.5–4.0                | 0.0–0.5              | 0.200               | no             | Hmt                                   | ND <sup>c</sup>            | 56%     |
| CH-11A  | 140              | 24 hr    | 3.5–4.0                | 1.0–1.5              | 0.020               | no             | Hmt                                   | 0.26                       | 91%     |
| CH-11B  | 140              | 24 hr    | 3.5–4.0                | 1.0–1.5              | 0.020               | no             | Hmt                                   | 0.20                       | 81%     |
| CH-10A  | 115              | 48 hr    | 3.5–4.0                | 0.0–0.5              | 0.200               | no             | Hmt                                   | 0.27                       | 56%     |
| CH-10B  | 115              | 48 hr    | 3.5–4.0                | 0.0–0.5              | 0.200               | no             | Hmt                                   | 0.30                       | 56%     |
| CH-9B   | 115              | 48 hr    | 3.5–4.0                | 1.0–1.5              | 0.020               | no             | Hmt                                   | 0.18                       | 100%    |
| CH-13A  | 95               | 182 hr   | 3.5–4.0                | 1.5–2.0              | 0.020               | no             | Hmt                                   | 0.12                       | 29%     |
| CH-13B  | 95               | 182 hr   | 3.5–4.0                | 1.5–2.0              | 0.020               | no             | Hmt                                   | ND                         | 22%     |
| CH-14A  | 95               | 90 hr    | 3.5–4.0                | 0.5                  | 0.200               | no             | Hmt + Akag                            | 0.33 (Hmt)                 | 32%     |
| CH-14B  | 95               | 182 hr   | 3.5–4.0                | 1.0–1.5              | 0.200               | no             | Akag + minor Hmt                      | 0.48                       | 36%     |
| CG-11A  | 70               | 217 hr   | 3.5–4.0                | 1.0–1.5              | 0.100               | no             | Akag                                  | ND                         | 42%     |
| CG-7A   | 50               | 37 days  | 3.5–4.0                | 1.0–1.5              | 0.100               | no             | Akag                                  | 0.57                       | 17%     |
| CG-7B   | 50               | 37 days  | 3.5–4.0                | 1.0–1.5              | 0.100               | no             | (Akag)                                | ND                         | 16%     |
| CG-9A   | 35               | 90 days  | 3.5–4.0                | 1.5–2.0              | 0.100               | no             | Akag                                  | 0.67                       | 13%     |
| CG-9B   | 35               | 90 days  | 3.5–4.0                | 1.5–2.0              | 0.100               | no             | (Akag)                                | ND                         | 10%     |
| NaOH experiment (OH/Fe ≈ 9)                                 |                  |          |                        |                      |                     |                |                                       |                            |         |
| CH-18A  | 140              | 24 hr    | >14.0                  | >14.0                | 0.050               | yes            | Gth + minor Hmt                       | 0.16                       | 100%    |
| CH-18B  | 140              | 24 hr    | >14.0                  | >14.0                | 0.050               | yes            | Gth + minor Hmt                       | 0.17                       | 99%     |
| CG-15A  | 115              | 48 hr    | >14.0                  | >14.0                | 0.050               | yes            | Gth                                   | 0.20                       | 93%     |
| CG-15B  | 115              | 48 hr    | >14.0                  | >14.0                | 0.050               | yes            | Gth                                   | 0.19                       | 89%     |
| CG-16A  | 95               | 140 hr   | >14.0                  | >14.0                | 0.050               | yes            | Gth                                   | 0.17                       | 96%     |
| CG-16B  | 95               | 140 hr   | >14.0                  | >14.0                | 0.050               | yes            | (Gth)                                 | ND                         | 97%     |
| CG-10A  | 70               | 217 hr   | >14.0                  | >14.0                | 0.050               | yes            | Gth                                   | ND                         | 102%    |
| CG-10B  | 70               | 217 hr   | >14.0                  | >14.0                | 0.050               | yes            | Gth                                   | ND                         | 99%     |
| CG-6A   | 50               | 37 days  | >14.0                  | >14.0                | 0.050               | yes            | Gth                                   | 0.26                       | 101%    |
| CG-6B   | 50               | 37 days  | >14.0                  | >14.0                | 0.050               | yes            | (Gth)                                 | ND                         | 101%    |
| CG-8A   | 35               | 90 days  | >14.0                  | >14.0                | 0.050               | yes            | Gth                                   | 0.27                       | 101%    |
| CG-8B   | 35               | 90 days  | >14.0                  | >14.0                | 0.050               | yes            | (Gth)                                 | ND                         | 99%     |
| NaOH + HCO <sub>3</sub> <sup>-</sup> experiment (OH/Fe ≈ 3) |                  |          |                        |                      |                     |                |                                       |                            |         |
| CH-16A  | 140              | 24 hr    | 8.0–8.5                | 9.0–9.5              | 0.114               | yes            | Hmt                                   | 0.21                       | 98%     |
| CH-16B  | 140              | 24 hr    | 8.0–8.5                | 9.0–9.5              | 0.114               | yes            | (Hmt)                                 | ND                         | 98%     |
| CH-17A  | 115              | 48 hr    | 8.0–8.5                | 9.0–9.5              | 0.114               | yes            | Hmt                                   | 0.22                       | 100%    |
| CH-15A  | 95               | 48 hr    | 8.0–8.5                | 9.5                  | 0.114               | yes            | Hmt                                   | 0.21                       | 100%    |
| CH-15B  | 95               | 48 hr    | 8.0–8.5                | 8.0–8.5              | 0.114               | yes            | Hmt                                   | 0.24                       | 100%    |
| CG-12A  | 70               | 217 hr   | 8.0–8.5                | 8.0                  | 0.114               | yes            | Hmt                                   | 0.30                       | 91%     |
| CG-12B  | 70               | 217 hr   | 8.0–8.5                | 8.0                  | 0.114               | yes            | Hmt                                   | 0.23                       | 90%     |
| CG-13A  | 50               | 315 hr   | 8.0–8.5                | 7.8                  | 0.114               | yes            | Hmt                                   | 0.26                       | 87%     |
| CG-13B  | 50               | 315 hr   | 8.0–8.5                | 8.0                  | 0.114               | yes            | Hmt                                   | 0.28                       | 89%     |
| CH-19A  | 37               | 189 days | 8.0                    | 8.8                  | 0.114               | yes            | Hmt + trace Gth?                      | 0.28                       | ND      |
| CH-19B  | 37               | 189 days | 8.0                    | 8.8                  | 0.114               | yes            | (Hmt + trace Gth?)                    | ND                         | ND      |
| CH-20A  | 30               | 189 days | 8.0                    | 8.8                  | 0.114               | yes            | Hmt                                   | 0.30                       | ND      |
| CH-20A*   | 30               | 190 days | 8.0                    | 8.8                  | 0.114               | no             | Hmt                                   | 0.41                       | ND      |
| CH-20B  | 30               | 189 days | 8.0                    | 8.8                  | 0.114               | yes            | (Hmt)                                 | ND                         | ND      |

<sup>a</sup> Gth, Hmt, and Akag are goethite, hematite, and akaganeite, respectively. Mineral phase in parenthesis indicates no XRD data were available. Mineralogy is estimated from similarity in color to its duplicate.

<sup>b</sup> FWHM is for full width at half-height maximum, a measure of crystallinity. Measured peaks are (110) for goethite, (104) for hematite, and (310) for akaganeite.

<sup>c</sup> Not determined.

the NaOH experiments, and oxygen from NaHCO<sub>3</sub> is ~0.4% of the total oxygen in the NaOH + HCO<sub>3</sub><sup>-</sup> experiments.

In Fh-exchange experiments, the δ<sup>18</sup>O values of solutions shifted during the course of aging (Table 4). These small shifts are expected because Fh gels contained a large amount of water that had a different δ<sup>18</sup>O value from that of two of the three aging solutions. For example, when Fh was placed in an aging solution with a higher δ<sup>18</sup>O value (+1.8‰), the δ<sup>18</sup>O of the bulk aging solution was decreased because of the contribution of a small amount of the -8.0‰ water from which the Fh was formed. Therefore, the δ<sup>18</sup>O value of the final solution was used to calculate α values.

### 3.5. Oxygen Isotope Composition of Ferric Oxides

Isotopic data and corresponding 1000lnα values are given for the three experiments in Table 5. It is clear that different ferric oxide phases have slightly different α-T relations (Fig. 1). The following observations are made from our three synthesis experiments:

1. 1000lnα values for goethite-water from the NaOH experiments were 0.7 to 3‰ more negative than those for hematite-water from the chemically similar NaOH + HCO<sub>3</sub><sup>-</sup> experiments. The difference was greater at lower temperatures.

Table 3. Contents of oxalate-extractable ferric oxides from precipitates of selected synthesis experiments.

| Sample name | Mineralogy <sup>a</sup> | Method   | Initial [Fe] (M) | Temperature (°C) | Duration | Oxalate-extractable (% weight) | Notes <sup>b</sup>   |
|-------------|-------------------------|--|------------------|------------------|----------|--------------------------------|--|
| Bu 1-3      | Akag                    | NaOH; OH:Fe = 12.5:1                               | 0.05             | 30               | 23 days  | 48.6%                          | Yapp's (1987) method 1, but with lower initial [Fe] (0.05 M instead of 0.09 M) |
| Bu 1-6      | Gth                     | NaOH; OH:Fe = 12.5:1                               | 0.05             | 61               | 23 days  | 2.7%                           | Yapp's (1987) method 1, but with lower initial [Fe] (0.05 M instead of 0.09 M) |
| Bu 2-6      | Fh? Gth?                | NaOH; OH:Fe = 2:1                                  | 0.05             | 61               | 23 days  | 5.7%                           | Yapp's (1987) method 2, but with lower initial [Fe] (0.05 M instead of 0.09 M) |
| Bu 3-6      | Gth + Hmt?              | Forced-hydrolysis                                  | 0.02             | 61               | 23 days  | 1.4%                           | Our own Forced-hydrolysis method   |
| Bu 5-6      | Gth + Hmt?              | Forced-hydrolysis                                  | 0.20             | 61               | 13 days  | 6.0%                           | Yapp's (1987) method 3   |
| Bu 4-3      | Hmt                     | NaOH + HCO <sub>3</sub> <sup>-</sup> ; OH:Fe = 3:1 | 0.11             | 30               | 23 days  | 54.3%                          | Our own NaOH + HCO <sub>3</sub> <sup>-</sup> method                            |
| Bu 4-6      | Hmt?                    | NaOH + HCO <sub>3</sub> <sup>-</sup> ; OH:Fe = 3:1 | 0.11             | 61               | 23 days  | 0.9%                           | Our own NaOH + HCO <sub>3</sub> <sup>-</sup> method                            |

<sup>a</sup> Judged from color.

<sup>b</sup> Fe(NO<sub>3</sub>)<sub>3</sub> and KOH were used in Yapp's (1987) experiments.

- 1000ln $\alpha$  values for goethite-water from the NaOH experiments were 1 to 2‰ more negative than those for akaganeite-water from the forced-hydrolysis experiments over the 35 to 70°C temperature range. The difference was greater at lower temperatures.
- Akaganeite-water from the forced-hydrolysis experiments and hematite-water from the NaOH + HCO<sub>3</sub><sup>-</sup> experiments had very similar 1000ln $\alpha$  values over the 35 to 70°C temperature range, with the former only ~0.2‰ more negative than the later.
- Over the 95° to 140°C temperature range, 1000ln $\alpha$  values for hematite-water from the NaOH + HCO<sub>3</sub><sup>-</sup> experiments were very close to those of hematite-water from the forced-hydrolysis experiments, with the former only 0.1 to 0.3‰ more negative than the later.
- In forced-hydrolysis experiments at 140°C, hematite obtained from solutions with initial [Fe<sup>3+</sup>] of 0.2 M had  $\delta^{18}\text{O}$  values ~0.5‰ more negative than those with initial [Fe<sup>3+</sup>] of 0.02 M. The same trend was observed at 115°C, but the 0.2 M hematites were only ~0.25‰ more negative, which is within the range of analytical error. The slightly more negative isotope fractionation in higher concentration so-

Table 4. Chemical conditions and oxygen isotope data for Fh-exchange experiments.

| Samples | Method (°C)                             | Duration | Solution pH |         | Mineral phase <sup>a</sup> | Solution $\delta^{18}\text{O}$ |       | $\delta^{18}\text{O}_{\text{ferric oxide predicted}}^b$ | $\delta^{18}\text{O}_{\text{ferric oxide measured}}^c$ | Oxygen exchanged <sup>d</sup> |
|---------|---|----------|-------------|---------|----------------------------|--------------------------------|-------|---|--|-------------------------------|
|         |   |          | initial     | final   |                            | initial                        | final |   |  |                               |
| CAG-1A  | OH + HCO <sub>3</sub> <sup>-</sup> (75) | 165 hr   | >14.0       | >14.0   | Gth                        | 1.8                            | 0.8   | -1.7  | -2.0   | 96.9%                         |
| CAG-1B  | OH + HCO <sub>3</sub> <sup>-</sup> (75) | 165 hr   | >14.0       | >14.0   | Gth                        | 1.8                            | 0.5   | -2.0  | -2.0   | 100.3%                        |
| CAG-2A  | OH + HCO <sub>3</sub> <sup>-</sup> (75) | 165 hr   | >14.0       | >14.0   | Gth                        | -8.0                           | -8.0  | -10.5   | -10.4  |                               |
| CAG-2B  | OH + HCO <sub>3</sub> <sup>-</sup> (75) | 165 hr   | >14.0       | >14.0   | Gth                        | -8.0                           | -8.0  | -10.5   | -10.0  |                               |
| CAG-3A  | OH + HCO <sub>3</sub> <sup>-</sup> (75) | 165 hr   | >14.0       | >14.0   | Gth                        | -15.1                          | -14.2 | -16.7   | -16.4  | 94.7%                         |
| CAG-3B  | OH + HCO <sub>3</sub> <sup>-</sup> (75) | 165 hr   | >14.0       | >14.0   | Gth                        | -15.1                          | -13.7 | -16.2   | -16.1  | 97.8%                         |
| CAG-4A  | HCO <sub>3</sub> <sup>-</sup> (75)      | 47 hr    | 8.0-8.5     | 9.0-9.5 | Hmt                        | 1.8                            | 0.8   | -0.1  | -0.6   | 93.9%                         |
| CAG-4B  | HCO <sub>3</sub> <sup>-</sup> (75)      | 47 hr    | 8.0-8.5     | 9.5     | Hmt                        | 1.8                            | 0.8   | -0.1  | -0.3   | 97.3%                         |
| CAG-5A  | HCO <sub>3</sub> <sup>-</sup> (75)      | 47 hr    | 8.0-8.5     | 9.5     | Hmt                        | -8.0                           | -8.0  | -8.9  | -8.6   |                               |
| CAG-5B  | HCO <sub>3</sub> <sup>-</sup> (75)      | 47 hr    | 8.0-8.5     | 9.5     | Hmt                        | -8.0                           | -8.0  | -8.9  | -8.5   |                               |
| CAG-6A  | HCO <sub>3</sub> <sup>-</sup> (75)      | 47 hr    | 8.0-8.5     | 9.0-9.5 | Hmt                        | -15.1                          | -14.3 | -15.2   | -14.9  | 95.8%                         |
| CAG-6B  | HCO <sub>3</sub> <sup>-</sup> (75)      | 47 hr    | 8.0-8.5     | 9.5     | Hmt                        | -15.1                          | -14.2 | -15.1   | -14.5  | 90.9%                         |
| CAG-7A  | HCO <sub>3</sub> <sup>-</sup> (30)      | 164 days | 8.0-8.5     | 9.2     | Hmt (minor Gth)            | 1.8                            | 0.9   | 2.0   | -0.2   | 75.7% <sup>e</sup>            |
| CAG-7B  | HCO <sub>3</sub> <sup>-</sup> (30)      | 164 days | 8.0-8.5     | 9.2     | Hmt (minor Gth)            | 1.8                            | 1     | 2.1   | 0.1  | 78.2% <sup>e</sup>            |
| CH-20A  | HCO <sub>3</sub> <sup>-</sup> (30)      | 189 days | 8.0-8.5     | 8.8     | Hmt                        | -8.0                           | -8.0  | -6.9  | -6.8   |                               |
| CH-20B  | HCO <sub>3</sub> <sup>-</sup> (30)      | 189 days | 8.0-8.5     | 8.8     | Hmt                        | -8.0                           | -8.0  | -6.9  | -6.9   |                               |
| CAG-8A  | HCO <sub>3</sub> <sup>-</sup> (30)      | 164 days | 8.0-8.5     | 9.2     | Hmt (minor Gth)            | -15.1                          | -14.4 | -13.3   | -13.6  | 104.1% <sup>e</sup>           |
| CAG-8B  | HCO <sub>3</sub> <sup>-</sup> (30)      | 164 days | 8.0-8.5     | 9.2     | Hmt (minor Gth)            | -15.1                          | -14.4 | -13.3   | -13.7  | 105.7% <sup>e</sup>           |

<sup>a</sup> Gth, Hmt, and Akag are goethite, hematite, and akaganeite, respectively.

<sup>b</sup> Calculated using equations in Fig. 1c and in Fig. 1d for goethite and hematite, respectively, and the  $\delta^{18}\text{O}$  of the final solution.

<sup>c</sup>  $\delta^{18}\text{O}$  value is the average of two duplicates for each sample, except for samples CAG-8B and CH-20B, which were single analyses. The difference between duplicate analyses is <0.3‰.

<sup>d</sup> Calculated assuming the completely exchanged fraction has the predicted value and the non-exchanged fraction has a  $\delta^{18}\text{O}$  value in equilibrium with water of -8.0‰.

<sup>e</sup> Calculated as 100% hematite. If calculated assuming 80% of the oxygen was from hematite and 20% from goethite, the predicted  $\delta^{18}\text{O}$  values are 1.4‰, 1.5‰, -13.9‰, and -13.9‰, and the exchange ratio is 81.9%, 84.3%, 95.5%, and 97.0% for sample CAG-7A, CAG-7B, CAG-8A, and CAG-8B, respectively.

Table 5. Oxygen isotope data for ferric oxides from three synthesis experiments.

| Sample <sup>a</sup>                             | <i>t</i> °C | Initial [Fe <sup>3+</sup> ]<br>(M) | Mineralogy       | δ <sup>18</sup> O | 1000lnα<br>(ferric oxide-water) |
|---|-------------|------------------------------------|------------------|-------------------|---------------------------------|
| Hydrolysis experiment                           |             |                                    |                  |                   |                                 |
| CH-12A-a  | 140         | 0.20                               | Hmt              | -10.3             | -2.3                            |
| CH-12A-b  | 140         | 0.20                               | Hmt              | -10.4             | -2.4                            |
| CH-12B-a  | 140         | 0.20                               | Hmt              | -10.6             | -2.6                            |
| CH-12B-b  | 140         | 0.20                               | Hmt              | -10.9             | -2.9                            |
| CH-11A-a  | 140         | 0.02                               | Hmt              | -10.2             | -2.2                            |
| CH-11A-b  | 140         | 0.02                               | Hmt              | -10.1             | -2.1                            |
| CH-11B-a  | 140         | 0.02                               | Hmt              | -9.9              | -1.9                            |
| CH-10A-a  | 115         | 0.20                               | Hmt              | -10.0             | -2.0                            |
| CH-10B-a  | 115         | 0.20                               | Hmt              | -10.0             | -2.0                            |
| CH-9B <sup>b</sup>                              | 115         | 0.02                               | Hmt              | -9.7              | -1.7                            |
| CH-14A-a  | 95          | 0.20                               | Hmt + Akag       | -9.2              | -1.2                            |
| CH-14A-b  | 95          | 0.20                               | Hmt + Akag       | -9.2              | -1.2                            |
| CH-14B-a  | 95          | 0.20                               | Akag + minor Hmt | -9.4              | -1.4                            |
| CH-13A-a  | 95          | 0.02                               | Hmt              | -9.2              | -1.2                            |
| CH-13B-a  | 95          | 0.02                               | Hmt              | -9.2              | -1.2                            |
| CG-11A-a  | 70          | 0.10                               | Akag             | -8.8              | -0.8                            |
| CG-7A-a   | 50          | 0.10                               | Akag             | -8.1              | -0.1                            |
| CG-7A-b   | 50          | 0.10                               | Akag             | -8.0              | 0.0                             |
| CG-7B-a   | 50          | 0.10                               | Akag             | -8.1              | -0.1                            |
| CG-9A-a   | 35          | 0.10                               | Akag             | -7.2              | 0.8                             |
| CG-9A-b   | 35          | 0.10                               | Akag             | -7.6              | 0.4                             |
| CGt-9B-a  | 35          | 0.10                               | Akag             | -7.3              | 0.7                             |
| NaOH experiment                                 |             |                                    |                  |                   |                                 |
| CH-18A-a  | 140         | 0.05                               | Gth + minor Hmt  | -11.8             | -3.8                            |
| CH-18A-b  | 140         | 0.05                               | Gth + minor Hmt  | -11.4             | -3.4                            |
| CH-18B-a  | 140         | 0.05                               | Gth + minor Hmt  | -11.2             | -3.2                            |
| CG-15A-a  | 115         | 0.05                               | Gth              | -11.2             | -3.2                            |
| CG-15B-a  | 115         | 0.05                               | Gth              | -11.1             | -3.1                            |
| CG-16A-a  | 95          | 0.05                               | Gth              | -10.7             | -2.7                            |
| CG-16A-b  | 95          | 0.05                               | Gth              | -10.6             | -2.6                            |
| CG-16B-a  | 95          | 0.05                               | Gth              | -10.7             | -2.7                            |
| CG-10A-a  | 70          | 0.05                               | Gth              | -10.5             | -2.5                            |
| CG-10B-a  | 70          | 0.05                               | Gth              | -10.5             | -2.5                            |
| CG-6A-a   | 50          | 0.05                               | Gth              | -10.0             | -2                              |
| CG-6A-b   | 50          | 0.05                               | Gth              | -10.2             | -2.2                            |
| CG-6B-a   | 50          | 0.05                               | Gth              | -10.3             | -2.3                            |
| CG-8A-a   | 35          | 0.05                               | Gth              | -9.6              | -1.6                            |
| CG-8B-a   | 35          | 0.05                               | Gth              | -9.6              | -1.6                            |
| CG-8B-b   | 35          | 0.05                               | Gth              | -10.2             | -2.2                            |
| NaOH + HCO <sub>3</sub> <sup>-</sup> experiment |             |                                    |                  |                   |                                 |
| CH-16A-a  | 140         | 0.11                               | Hmt              | -10.5             | -2.5                            |
| CH-16A-b  | 140         | 0.11                               | Hmt              | -10.5             | -2.5                            |
| CH-16B-a  | 140         | 0.11                               | Hmt              | -10.5             | -2.5                            |
| CH-17A-a  | 115         | 0.11                               | Hmt              | -10.2             | -2.2                            |
| CH-15A-a  | 95          | 0.11                               | Hmt              | -9.9              | -1.9                            |
| CH-15A-b  | 95          | 0.11                               | Hmt              | -9.9              | -1.9                            |
| CH-15B-a  | 95          | 0.11                               | Hmt              | -9.5              | -1.5                            |
| CH-15B-b  | 95          | 0.11                               | Hmt              | -9.5              | -1.5                            |
| CG-12A-a  | 70          | 0.11                               | Hmt              | -8.6              | -0.6                            |
| CG-12B-a  | 70          | 0.11                               | Hmt              | -8.5              | -0.5                            |
| CG-13A-a  | 50          | 0.11                               | Hmt              | -7.8              | 0.3                             |
| CG-13A-b  | 50          | 0.11                               | Hmt              | -7.8              | 0.2                             |
| CG-13B-a  | 50          | 0.11                               | Hmt              | -7.8              | 0.2                             |
| CH-19A-a  | 37          | 0.11                               | Hmt + trace Gth? | -7.7              | 0.3                             |
| CH-19A-b  | 37          | 0.11                               | Hmt + trace Gth? | -7.7              | 0.3                             |
| CH-20A-a  | 30          | 0.11                               | Hmt              | -6.9              | 1.1                             |
| CH-20A-b  | 30          | 0.11                               | Hmt              | -6.7              | 1.3                             |
| CH-20B-a  | 30          | 0.11                               | Hmt              | -6.9              | 1.1                             |
| CH-20A*-a <sup>c</sup>                          | 30          | 0.11                               | Hmt + trace Gth  | -5.1              | 2.9                             |
| CH-20A*-b                                       | 30          | 0.11                               | Hmt + trace Gth  | -5.3              | 2.7                             |

<sup>a</sup> A and B are bottle duplicates of the same experiment; a, b, c, d are isotope analyses of replicates from precipitate of the same bottle. Most bottles have two or more isotope analyses. A few bottles have only one value reported due to analytical failure.

<sup>b</sup> Average value of >15 replicates, analyzed as reference in this study.

<sup>c</sup> Precipitate from the bottle of CH-20A, but dried in 100°C oven without HCl rinse.

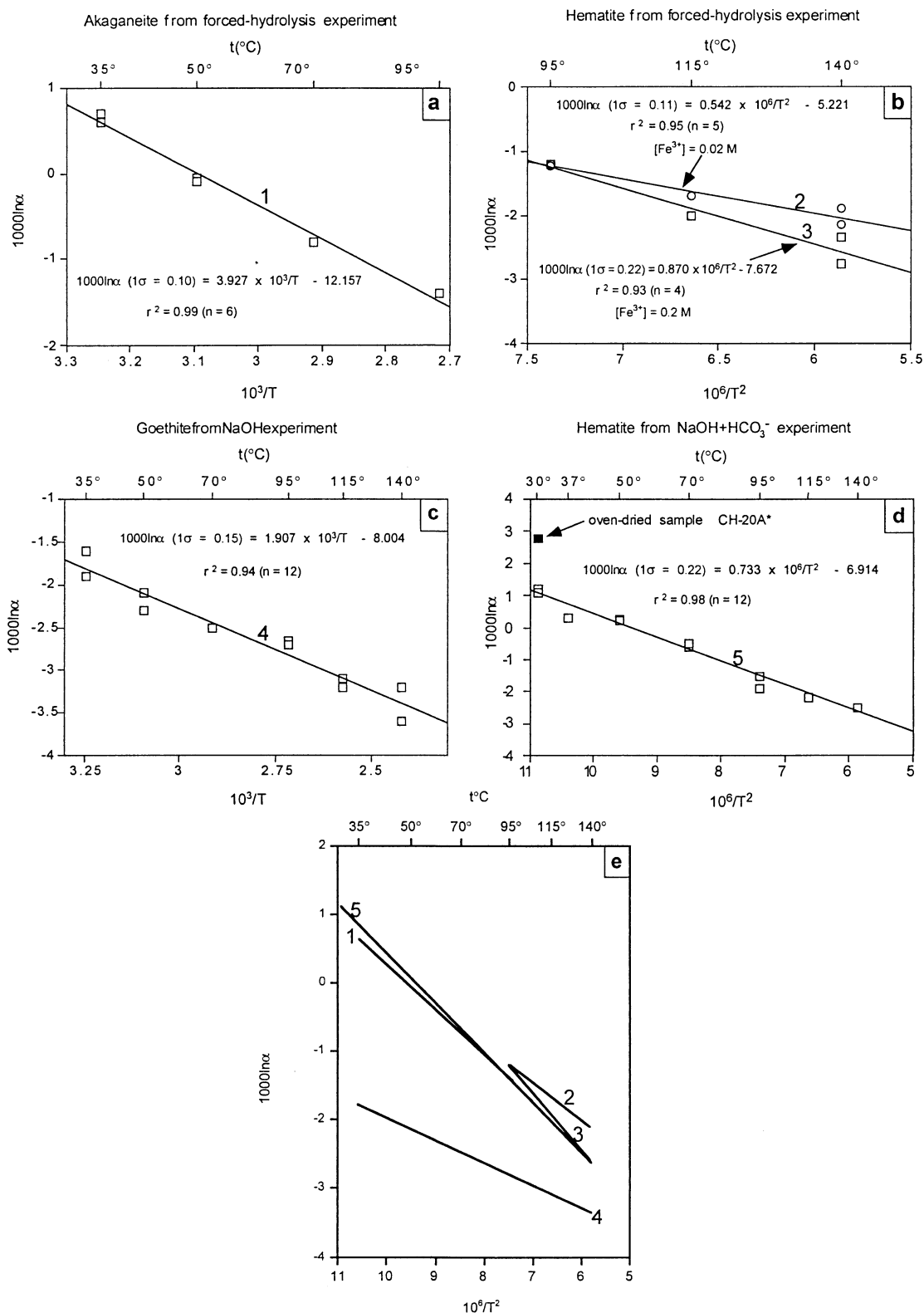


Fig. 1. Temperature dependence of oxygen isotope fractionation between ferric oxides (akaganeite, hematite, and goethite) and water in three synthesis experiments. The regressions are plotted and calculated using average values for replicate fluorinations of single bottles. In Fig. 1a, only sample "CH-14B-c" is used for the 95°C in the akaganeite-water regression. Comparison of the  $\alpha$ - $T$  relation for our different experiments is shown in Fig. 1e, where the fitting lines for goethite-water and akaganeite-water are against " $10^6/T^2$ " rather than " $10^3/T$ " as in Fig. 1a and Fig. 1c. There is essentially no difference in the fitting lines when either " $10^6/T^2$ " or " $10^3/T$ " is used as variable across the narrow range of temperature.

lutions is associated with a reduced yield in these experiments.

- Samples from the  $\text{NaOH} + \text{HCO}_3^-$  experiment that were not HCl treated and were oven-dried had  $\delta^{18}\text{O}$  values 1.6‰ higher than acid-treated, vacuum-dried samples. It seems that different cleaning and drying methods had a major effect on the measured  $\delta^{18}\text{O}$  of ferric oxides.

The Fh-exchange experiments yielded intriguing results as well (Table 4). The measured  $\delta^{18}\text{O}$  values for goethite and hematite at a particular temperature were close to the values predicted using the  $\delta^{18}\text{O}$  value of final aging solutions and the fractionation equations established above. This result suggests that newly formed hematite and goethite exchanged oxygen with the later aging solutions, rather than inheriting oxygen from Fh that had exchanged with initial source water. However, the  $\delta^{18}\text{O}$  values of ferric oxides are not exactly the same as predicted for the two sets of experiments in which the  $\delta^{18}\text{O}$  values of the aging solutions were different from that of the Fh source solution ( $-8.0\text{‰}$ ). In particular, measured  $\delta^{18}\text{O}$  values of ferric oxide from the high- $\delta^{18}\text{O}$  aging solutions (1.8‰) were lower than predicted, whereas those from the low- $\delta^{18}\text{O}$  aging solution ( $-15.1\text{‰}$ ) were higher than predicted. As discussed below, we believe that this discrepancy is caused by unsuccessful dispersion of some of the Fh aggregates, which results in uncompleted exchange with ambient water.

#### 4. DISCUSSION

##### 4.1. Comparison to the Results of Prior Synthesis Experiments

The most salient feature of our results is their difference from Eqn. 2, the fractionation relation determined by Yapp (1990a), regardless of the mineral phase or synthetic method (Figs. 1, 2). Except at the highest temperatures, our  $1000\ln\alpha$  is always lower in value and less sensitive to temperature than those calculated by Eqn. 2, particularly for goethite from strongly alkaline solutions.

Goethite was synthesized via three different methods in Yapp's (1987) experiments. His methods 1 and 2 are similar to our NaOH experiments, except that he used  $\text{Fe}(\text{NO}_3)_3$  rather than  $\text{FeCl}_3$  and KOH rather than NaOH. The OH/Fe ratio was 12.5 in his method 1, and 2 in method 2. Yapp's method 3 is similar to our forced-hydrolysis experiment but with 10 times higher initial  $[\text{Fe}^{3+}]$ . After being soaked in DD water for 22 to 96 days to clean the nitrate, samples obtained by methods 2 and 3 were used to determine the goethite-water oxygen isotope fractionation, because of the concern that more slowly precipitated goethites from his methods 2 and 3 may approach isotopic equilibrium between mineral and water more closely than the rapidly precipitated goethite from his method 1. We notice, however, that the two goethite samples (SG-8-2 and SG-7-1 at  $62^\circ\text{C}$  and  $25^\circ\text{C}$ , respectively) from Yapp's (1987) method 1, which is similar to our NaOH experiment, had  $1000\ln\alpha$  values relatively close to our experimental results, although these values are still 1.5 to 2.5‰ more positive than ours.

Hematite syntheses in Yapp's (1990a) experiments were undertaken at  $62^\circ$ ,  $92^\circ$ , and  $120^\circ\text{C}$ . The  $62^\circ\text{C}$  experiment proceeded by method 2 (OH/Fe = 2), and it produced a mixture of hematite and goethite. The  $92^\circ$  and  $120^\circ\text{C}$  experiments

proceeded by a forced-hydrolysis method (method 3), and they produced only hematite. While the hematite from the  $120^\circ\text{C}$  experiment had a  $1000\ln\alpha$  value nearly identical to our forced-hydrolysis experimental result, the values for the  $95^\circ\text{C}$  and  $62^\circ\text{C}$  experiments were 1‰ and 2.5‰ more positive than ours, respectively. Plots of oxygen isotope fractionation factors versus temperature for hematite and goethite from Yapp's experiments could be fit cleanly by a single straight line, from which it was concluded that hematite and goethite had the same oxygen isotope fractionation factors at temperatures ranging from  $25^\circ$  to  $120^\circ\text{C}$ . This combined relation (Eqn. 2) has a temperature-sensitivity of  $\sim 0.14\text{‰}$  per  $^\circ\text{C}$ , which is much higher than the 0.02 to 0.03‰ per  $^\circ\text{C}$  from this study.

In Müller's (1995) synthesis study, the KOH-method was essentially the same as our NaOH experiment with an OH/Fe ratio of  $\sim 9$ . As in our experiments, all precipitates were exclusively goethite. Müller's NaOH and hydrolysis methods were similar to Yapp's (1987) methods 2 and 3, respectively. One difference is that in Müller's NaOH-method the OH/Fe ratio was changed from 3 at  $20^\circ\text{C}$  to 2 at  $60^\circ\text{C}$ , rather than being kept at 2 as in Yapp's method 2. No specific information about the mineralogy of the precipitates were given by Müller (1995) for the NaOH and hydrolysis experiments.

As shown in Fig. 2, the  $\alpha$ - $T$  curve from Müller's KOH experiment intersects the curve from our NaOH experiments at  $65^\circ\text{C}$ , but has a steeper slope. Müller's NaOH experiment produced an  $\alpha$ - $T$  curve nearly identical to that generated from our NaOH experiments in slope, but  $\sim 2\text{‰}$  more positive. The most unusual feature of Müller's experiments is the  $\alpha$ - $T$  relation obtained from his hydrolysis experiment, which had a relatively steep slope that differed greatly from that of his two alkaline synthesis experiments. Interestingly, the  $\alpha$ - $T$  relation generated from Müller's hydrolysis experiments are most similar to Eqn. 2, which Yapp (1987, 1990a) derived from several different methods.

##### 4.2. Assessment of Isotopic Equilibrium

Two factors are often called upon to explain discrepancies among low temperature mineral-water isotope fractionation curves. First, it is often argued that different chemical conditions and formation pathways may result in different  $\alpha$ - $T$  relations for experimental products. Vague terms like "isotopic inheritance" are sometimes used to explain discrepancies if an intermediate phase is involved in mineral precipitation. Second, it is often difficult to demonstrate that low temperature synthesis experiments have attained isotopic equilibrium between the newly precipitated mineral phase and solution (O'Neil, 1986; Yapp, 1987; Savin and Lee, 1988; Sharp and Kirschner, 1994). In fact, both these factors are attributable to kinetic isotopic fractionation effects, which occur when the reaction involves incomplete, fast, and/or unidirectional processes (e.g., evaporation, diffusion, mineral precipitation, and enzyme-catalyzed reactions).

Crystal growth from aqueous solutions can be divided into three consecutive processes: (1) transport of ions from solution to the growing surface; (2) formation of a neutral species of the same stoichiometry as the solid at the surface; and (3) incorporation of this neutral species onto the surface (Walton, 1967). This heterogeneous reaction can be in chemical equilibrium

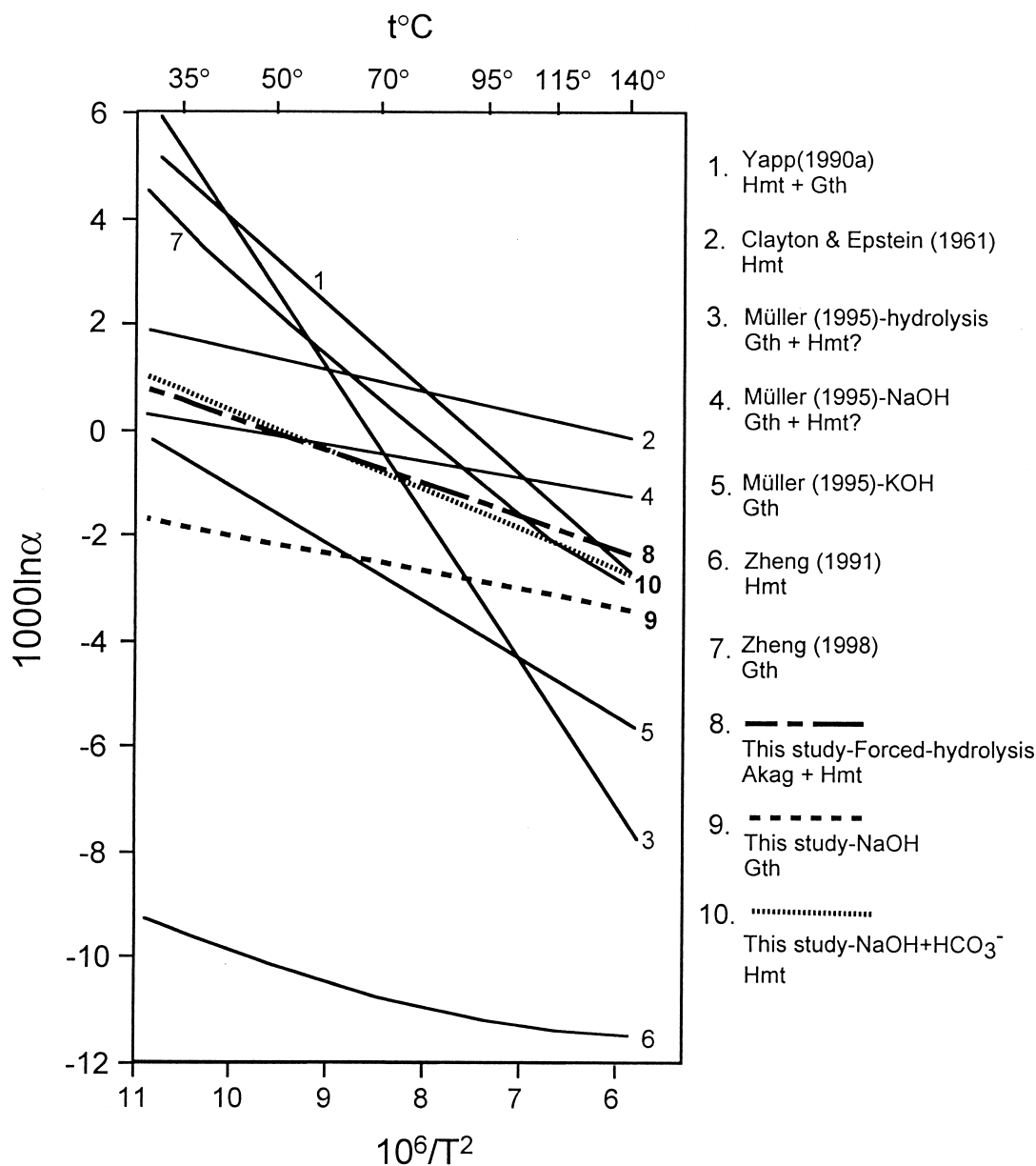


Fig. 2. Comparison of oxygen isotope fractionation-temperature relations in ferric oxide-water system from different studies. Hmt, Gth, and Akag are hematite, goethite, and akaganeite, respectively. Line 8 is obtained from all  $\delta^{18}\text{O}$  data of ferric oxides in forced-hydrolysis experiments, including both akaganeite and hematite phases.

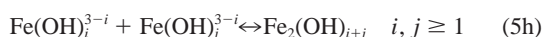
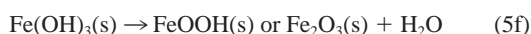
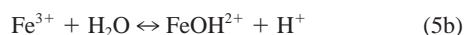
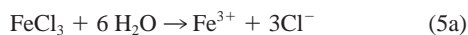
locally, but overall it is unidirectional in the sense that, as ions are incorporated onto the surface, they are covered by new layers of crystal, and are not able to exchange atoms with ambient solution (or more precisely, the rate of further exchange is extremely slow at surface temperatures). Kinetic isotope fractionations may occur during any of these steps, and the kinetic fractionation at the rate limiting step in the reaction series will determine the magnitude of kinetic isotope effect for the growing mineral.

The only method that can unambiguously demonstrate isotopic equilibrium between a mineral and a fluid are two-direction exchange reactions. Equilibrium is accepted if the

minerals approach the same isotopic composition following exchange from two different starting compositions, provided that no reprecipitation and recrystallization occur during the exchange processes. Low temperature synthesis experiments, on the other hand, are often questioned because isotopic equilibrium can be approached from only one direction during dissolution/reprecipitation in the mineral-water system (O'Neil, 1986). Unfortunately, the two-direction method is only feasible in high temperature (>500°C) experiments, because of the extremely low rates of exchange between mineral and water at low temperatures. While it may be impossible to determine experimentally if a mineral-water system has

reached isotopic equilibrium during low temperature synthesis, an evaluation of reaction kinetics, especially the rate-limiting steps, may reveal whether kinetic isotope effects are likely to be significant during mineral precipitation.

Fe(III) hydrolysis in ferric oxide-water systems involves mono-, di-, and poly-nuclear iron hydroxide ions. It consists of the following elementary steps (with inner-sphere water molecules omitted):



Precipitation of ferric oxides by hydrolysis starts with the formation of small ferric hydroxide polymers, progresses to larger polymers and colloidal solids, and eventually ceases when gels age to crystalline phases. Solution pH determines the dominant Fe(III) species. For example, solutions do not contain detectable amounts of polynuclear species and nucleation is heterogeneous when the molar ratio of  $\text{HCO}_3^-$  to Fe(III) ( $a$ ) is less than 0.6 ( $a < a_{\min}$ ,  $a_{\min} = 0.6$ ), whereas the solution is dominated by polynuclear species when  $a > a_{\min}$  and the nucleation is homogeneous (Schneider, 1984; Schneider and Schwyn, 1987). During our forced-hydrolysis experiments, precipitation probably occurred via the former pathway, as  $a = 0$ , whereas in the NaOH and NaOH +  $\text{HCO}_3^-$  experiments, the reactions most likely proceeded via the later pathway. The rates of hydrolysis of Fe(III) species and their exchange with ambient water (Eqns. 5b, 5c, 5d) are extremely rapid and are generally considered to exist at equilibrium at all times (Wendt, 1973; Grant and Jordan, 1981; Stumm and Morgan, 1981; Schneider and Schwyn, 1987; Grundl and Delwiche, 1993).

In most crystal growth processes, formation of a neutral species of the same stoichiometry as the solid on the surface of the crystal is the rate-limiting step. Recent investigations of ferric oxide precipitation from ferric solutions are consistent with a kinetic model in which precipitation of ferric solid from  $\text{Fe(OH)}_3^0$  (Eqn. 5e) is the rate limiting step (Grundl and Delwiche, 1993). In the ferric oxide-water system, the neutral species  $\text{Fe(OH)}_3^0$  is maintained in solution by the rapid hydrolysis of Fe(III), thus the formation of this neutral species does not limit the rate of crystal precipitation and growth. It is, therefore, quite likely that oxygen isotope equilibrium is rapidly established between water and dissolved species from Fe(III) to  $\text{Fe(OH)}_3^0$ .

Incorporation of this neutral species onto the crystal surface (Eqn. 5e) is highly dependent on solution conditions and is generally very slow at surface temperature (Van der Woude and De Bruyn, 1984). Early-formed, kinetically-stable phases are usually poorly ordered, and rapid growth to small polymers

(Eqn. 5h) is reversible (Dousma and De Bruyn, 1976). The critical nucleus of ferric oxide formation can be  $[\text{Fe(OH)}_3]^{4-}$  (Melikhov et al., 1987) or  $\text{Fe}_9(\text{OH})_{20}^{7+}$  (Van der Woude and De Bruyn, 1983). Further addition of precursor species  $\text{Fe(OH)}_3^0$  or  $\text{Fe}_3(\text{OH})_4^{5+}$  promotes crystal growth. The poorly ordered phase is sometimes referred to as a ferric gel or as the mineral ferrihydrite, and it may dissolve and reprecipitate later as a stable crystalline phase, or be transformed internally to become more ordered by the expulsion of  $\text{H}_2\text{O}$  molecules from its structure (Eqn. 5f). The poorly ordered phase may be quite accessible for further exchange of oxygen atoms with ambient water, as shown by our Fh-exchange experiment. Although a kinetic isotope effect can not be entirely ruled out for Eqn. 5f, this generally slow and initially reversible process is not likely to produce a significant kinetic isotope effect.

In summary, because the neutral species,  $\text{Fe(OH)}_3^0$ , rapidly exchanges oxygen with water and is maintained in solution, and because the incorporation of neutral species into the crystal is slow and reversible during the early stages of mineral formation, oxygen isotope fractionation in ferric oxide-water systems is unlikely to be highly-sensitive to different initial chemical conditions (i.e., kinetic isotope effect should be small). Equilibrium fractionation among hydrolytic species and at the crystal formation step are more likely in control. This conclusion is supported by the results of our synthesis experiments, which suggested nearly identical fractionation relations for hematite precipitated by two different experiments (NaOH +  $\text{HCO}_3^-$  and forced-hydrolysis) or from solutions with different initial  $[\text{Fe}^{3+}]$  that had different yields.

In our synthesis experiments, the fractionation relation for goethite-water was slightly different from those for hematite-water and akaganeite-water. This is not unexpected; these different ferric oxides have different crystal structures which may explain differences in fractionation. However, these differences are small and cannot explain the large discrepancies in  $\alpha$ - $T$  relations among prior experiments. Unless the expulsion of water from  $\text{Fe(OH)}_3$  (Eqn. 5f) has an extremely large kinetic isotopic effect depending on different reaction rates (which seems unlikely from the results of our study), there is no compelling theoretical explanation for the different oxygen isotope fractionation relations obtained in synthesis experiments by different authors. While not ruling out other potential explanations, we would like to point out one source for these discrepancies: the washing and drying procedures in experiment.

### 4.3. Importance of Proper Drying Procedures

Amorphous ferric gels and poorly-crystalline phases (e.g., Fh) are present in ferric oxide precipitates synthesized at low temperatures (Landa and Gast, 1973). If the non-structural waters are not washed or leached from the samples, they will transform into a stable ferric oxide phase with an oxygen isotope composition influenced by the  $^{18}\text{O}$ -enriched pore water generated by evaporation during oven-drying. Therefore, the increasingly positive  $\delta^{18}\text{O}$  values observed for ferric oxides synthesized at lower temperatures in some experiments may in part reflect the increasing amount of amorphous phase (and non-structural water) in final precipitates. Likewise, the different fractionation factors obtained via different synthetic path-

ways may partly result from differences in the amount of non-structural water in ferric oxides generated by the method. Bird et al. (1993) also mentioned that incompletely removed hydration water from some of their low temperature titanium-oxide precipitates may be a possible factor that contributed to error in derived  $\alpha$ - $T$  curve for the titanium oxide-water system.

Several lines of evidence are consistent with our speculation. First, amorphous and poorly-crystalline phases are present in significant amounts in low-temperature ferric oxide precipitates, as demonstrated by the percent of oxalate-extractable ferric oxides in various precipitates (Table 3). Second, ferrihydrite does transform into more crystalline goethite and hematite, as indicated by the appearance of goethite and hematite peaks in our XRD data upon drying in 50°C oven. Third, sample CH-20A\* had a  $\delta^{18}\text{O}$  value 1.6‰ higher than sample CH-20A. This difference is in the direction expected if evaporatively  $^{18}\text{O}$ -enriched waters were exchanged with amorphous and poorly-crystalline phases during their transformation to more stable ferric oxides.

We opted for HCl-washing rather than the usual oxalate-treatment because the former is fast and minor dissolution of crystalline ferric oxide would not affect our isotopic results. The HCl-washing method has been used to clean sodalite in a procedure of concentrating ferric oxide from soil clays (Singh and Gilkes, 1991). Furthermore, it has been shown by infrared spectroscopy that vacuum-drying removes adsorbed water from Fh almost completely, even at room temperature (Russell, 1979). We suggest, therefore, that to obtain reliable  $\delta^{18}\text{O}$  values for minerals that may contain amorphous and poorly-crystalline phases, acid washing and vacuum drying (preferably freeze-drying) prior to isotopic analysis are essential.

In our experiments, precipitates from forced-hydrolysis experiments were not treated with HCl, due to an early assumption that few amorphous phases would be produced during the heterogeneous nucleation processes. And even if a small amount of amorphous phase was present in these samples, vacuum-drying should have removed most adsorbed water from residual Fh in untreated samples. Since we do not have evidence demonstrating that amorphous and poorly-crystalline phases are completely removed from precipitates by our rigorous treatment regime, it is possible that some of the small but systematic differences in  $\delta^{18}\text{O}$  between ferric oxide precipitates synthesized at the same temperature by different methods could reflect differences in the concentrations of residual amorphous and poorly-crystalline phases, rather than fundamental differences in isotope fractionation related to mineral phases.

Acid-washing was not mentioned in the description of Müller's (1995) experiments. Samples were merely dried at 40°C for 48 hr prior to isotopic analysis. In Yapp's (1987, 1990a) experiments, precipitates were soaked in DD water with the same  $\delta^{18}\text{O}$  as synthesis and aging solutions for days or months. The  $\delta^{18}\text{O}$  of thoroughly rinsed goethite was systematically more negative than unrinsed goethite, which can be explained by the remove of nitrate or by an increased crystallinity (decreased amorphous content) after prolonged soaking. Drying procedures were not described in Yapp's papers.

In summary, we propose that differing contents of residual amorphous and poorly-crystalline phases in low temperature precipitates may be one of the factors responsible for the discrepancies in  $\alpha$ - $T$  relation for the same mineral phase.

Further experiments are needed, however, to test this hypothesis, and to quantify the effects of the content of amorphous and poorly-crystalline phases as well as the drying procedures on the  $\delta^{18}\text{O}$  of final precipitates.

#### 4.4. Comparison with Calculated Fractionation Relations

Clayton and Epstein (1961) inferred a hematite-water oxygen isotope fractionation relation of:

$$1000\ln\alpha = 0.413 \times 10^6/T^2 - 2.56 \quad (6)$$

from the  $\delta^{18}\text{O}$  of coexisting quartz, calcite, and hematite in hydrothermal deposits and the known calcite-water fractionation factor. This fractionation relation has a temperature sensitivity of 0.02‰ per °C from 30° to 100°C, very close to our experimental data, but it has a  $1000\ln\alpha$  value 1–2‰ more positive than ours at these temperatures. Since this relation was derived from measurements of mineral assemblages that had equilibrated naturally for a significant length of time, it is likely that it provides a good approximation for oxygen isotope fractionation for natural hematites. There are uncertainties regarding this relation, however, including: (1) the assumption that the  $\delta^{18}\text{O}$  of hydrothermal fluids does not change from high- to low-temperature hydrothermal systems; and (2) the extrapolation from hydrothermal temperatures to surface temperatures.

Semi-theoretical calibrations of oxygen isotope fractionation relations by Zheng (1991, 1998), estimated using a modified increment method, produced a hematite-water  $\alpha$ - $T$  relation of

$$1000\ln\alpha = 2.69 \times 10^6/T^2 - 12.82 \times 10^3/T + 3.78 \quad (7)$$

and a goethite-water  $\alpha$ - $T$  relation of

$$1000\ln\alpha = 3.31 \times 10^6/T^2 - 0.39 \times 10^3/T + 2.74 \quad (8)$$

These relations are drastically different from one another (Fig. 2). The calculated hematite-water relation exhibits little sensitivity to temperature, in agreement with our synthesis experiments, but much more negative  $1000\ln\alpha$  values at near surface temperatures than any other relations. Interestingly, the goethite-water relation (Eqn. 8) matches Yapp's (1990a) goethite/hematite-water relation (Eqn. 2) quite well. Uncertainty involving this semi-theoretical calibration is the lack of a systematic approach to determine the adjustable parameters in the method (Chacko et al., 1996; Polyakov and Ustinov, 1997).

Finally, while a careful discussion of oxygen isotope fractionation in the magnetite-water system is beyond the scope of this paper (Taylor, 1968; Becker and Clayton, 1976; Blattner et al., 1983), it should be noted that Clayton and Epstein (1958) concluded that  $1000\ln\alpha$  for this system is very close to zero from room temperature to several hundreds of °C, on the basis of a series of  $\delta^{18}\text{O}$  values for quartz-magnetite mineral pairs. Recent work by Zhang et al. (1997) on bacterially-precipitated, magnetite-enriched ferric oxides also produced a fractionation curve similar to our results for ferric oxides.

In summary, the oxygen isotope fractionation relations calculated from natural mineral assemblages are in good agreement with our experimental results. Although the modified increment method generated a slope for the  $\alpha$ - $T$  relation similar

to our experimental results, the absolute value of  $\alpha$  was significantly different.

#### 4.5. Implications of the Fh-exchange Experiments

Ferrihydrite is commonly found in soils, weathered rocks, sediments, and in aqueous systems. It is a ferric oxide that exhibits varying degrees of crystallinity, from two broad peaks in 2-line Fh to 6 peaks in 6-line Fh. Sometimes, 2-line Fh is referred to as an “amorphous” product, as the XRD patterns display few reflections. However, unlike glasses or amorphous metals, Fh is ordered at a local scale, and the lack of reflections is mainly due to the extremely small size of coherent scattering domains (Drits et al., 1993). Our air-dried Fh samples exhibit no distinct peaks and are most similar to 2-line Fh or a ferric hydrous gel.

Fh has long been regarded as the precursor for hematite, goethite, and akaganeite, yet the mechanisms of these structural transformations remain unclear. Extensive studies in solution chemistry have led to the hypothesis that the transformation proceeds via two competing pathways: (1) dissolution-reprecipitation; and (2) internal dehydration and solid-state rearrangement. The former pathway is thought to dominate in Fh-to-goethite transformations, whereas the latter is thought to occur during Fh-to-hematite transformations (Fischer and Schwertmann, 1975; Schwertmann and Murad, 1983). The structure of most crystalline ferric oxides can be described in terms of closely-packed stacks of oxygen atomic planes. Hematite is characterized by the presence of face-sharing Fe octahedra, a feature that is not present in  $\alpha$ -,  $\beta$ -, and  $\gamma$ -FeOOH structures. Recent studies using extended X-ray absorption fine structure (EXAFS) spectroscopy provide information about the defect structures of finely-dispersed Fh and ferric gels (Combes et al., 1990; Drits et al., 1993; Manceau and Drits, 1993). Structural models for Fh based on EXAFS include some face-sharing octahedra, rendering a direct transformation of ferric gel or Fh into goethite, without dissolution-reprecipitation, impossible. In contrast, Mössbauer spectral data support the hypothesis of a direct transformation of Fh to hematite by the coalescence of Fh particles (Johnston and Lewis, 1983). Yet the Fh structure model derived from EXAFS does not fully support a solid-state mechanism for the Fh-to-hematite transformation. Manceau and Drits (1993) note:

... the transformation of Fh proper to hematite again necessitates the moving of O atoms belonging to Fh proper from C to B position, and thus dissolving the Fh proper component. That the formation of hematite and goethite from Fh appears macroscopically to follow two different pathways can be accounted for by the fact that these two transformations differ in the extent to which the dissolution-reprecipitation process affects the ferrihydrite framework. This process would operate solely during the formation of goethite, whereas both dissolution and the solid-state transformation would take place during the formation of hematite (p. 182).

In our Fh-exchange experiments, it is apparent that the exchange of oxygen between Fh and the aging solution, which has a different  $\delta^{18}\text{O}$  composition than the solution from which Fh initially formed, is nearly complete (Table 4). The systematic shift (0.1–0.6‰) in 75°C experiments towards the  $\delta^{18}\text{O}$  of the initial solution from which Fh was formed is most likely caused by the many small Fh aggregates we observed in aging

solutions. Unlike the other synthesis experiments, which have homogeneous and well dispersed precipitates, the Fh-exchange experiment is found to contain aggregates which were difficult to disperse during the course of aging. The presence of these aggregates may limit complete exchange of oxygen atoms between solutions and the Fh inside the aggregates. Thus a small portion (~4–10%) of the original Fh  $\delta^{18}\text{O}$  signal is retained by crystals, resulting in a positive shift for crystals in the more  $^{18}\text{O}$ -depleted aging solutions and a negative shift for crystals in the more  $^{18}\text{O}$ -enriched aging solutions. We do not think that the retention of these small fractions of original Fh isotopic signal is the result of partial solid-state transformation during the Fh aging processes. Hematite and goethite exhibit a similar shift, yet it is less controversial and well-accepted that goethite formation from Fh is via dissolution-reprecipitation.

At first inspection, the trend in the 30°C exchange experiments appears to refute the explanation above, since measured  $\delta^{18}\text{O}$  values of precipitates from both the –15.1‰ and the 1.8‰ aging solutions are more negative than predicted, and the shift in the 1.8‰ solution is as large as –2‰ (Table 4). However, hematite produced from both solutions has a minor goethite component, and our synthesis results indicate that goethite will have a  $\delta^{18}\text{O}$  value ~3‰ more negative than hematite at 30°C. The shift caused by the goethite component could be precisely calculated if the goethite/hematite ratio were known accurately in our samples. Nevertheless, the magnitude and direction of the deviations can be explained when the influences of both aggregates and the goethite component are considered.

Our observations provide strong support for Manceau and Drits' (1993) proposal that dissolution and reprecipitation also occur during the Fh-to-hematite transformation. However, our results do not firmly indicate the presence of partial solid-state transformation in the 2-line-Fh to hematite transformation. As our experiments start from very poorly ordered 2-line Fh, further study on more ordered 6-line Fh might provide more information on differences in potential mechanisms for the Fh-to-crystalline oxide transformation.

#### 4.6. Implications for Paleoclimatic and Diagenetic Studies

Our synthesis experiments demonstrate that the temperature-sensitivity of oxygen isotopic fractionation in ferric-water systems is among the lowest known for minerals under near surface conditions. The oxygen isotope composition of ferric oxide is very close to that of the water from which the ferric oxide precipitated or aged. This attribute makes the ferric oxide-water systems useful for studies on the oxygen isotope chemistry of ancient surface waters, as uncertainties regarding surface temperature will have little impact on the reconstructed water  $\delta^{18}\text{O}$  value.

Another distinctive feature of ferric oxides is the long aging process required before they become stable, highly-crystalline mineral phases under surface conditions. In nature, the primary products of the oxygenation of Fe(II) at an oxic-anoxic boundary are polynuclear aggregates of Fe(III) hydroxides and Fh (Schwertmann and Fischer, 1973; von Gunten and Schneider, 1991). The results of our Fh-exchange experiment imply that the oxygen isotope composition of natural ferric oxides reflects

equilibration with a long term average for local environmental water. Short-term variations in the oxygen isotope composition of ambient water are unlikely to be preserved, owing to the slow and open transformation processes from metastable to stable ferric oxide phases. In particular, the  $\delta^{18}\text{O}$  of average meteoric water may be recorded by ferric oxides if they were buried after formation. Once crystallized, ferric oxides retain their original isotopic composition with high fidelity (Becker and Clayton, 1976; Yapp, 1991).

## 5. CONCLUSIONS

The results of our synthesis experiments reveal that, at near surface temperatures, oxygen isotope fractionations in ferric oxide-water systems are small, with the lowest temperature sensitivity for any commonly occurring mineral-water system. Hematite and goethite exhibit subtly different  $\alpha$ - $T$  relations with water, with goethite more negative than hematite by 1 to 2.5‰ at all temperatures. The same phase formed by different pathways or from different initial  $[\text{Fe}^{3+}]$  solutions shows no significant difference in  $\alpha$ - $T$  relation.

The discrepancies among  $\alpha$ - $T$  relations obtained by different research groups for ferric oxide-water systems can not be explained solely by differences in chemical conditions or formation pathways. One explanation for these discrepancies may be differences in sample washing and drying procedures. The transformation from poorly-ordered ferrihydrite to crystalline hematite or goethite is an open process in terms of oxygen isotope exchange between minerals and ambient water. The combination of two attributes, the low temperature-dependence of oxygen isotope fractionation and the continuous isotopic exchange with ambient fluids over several thousands of years, makes ferric oxides ideal proxies for the  $\delta^{18}\text{O}$  of ancient fluids in paleoclimatic and paleohydrologic research.

*Acknowledgments*—Earlier discussions with J. M. Bigham and P. H. Hsu were most helpful. We thank D. Rumble III for assistance in oxygen isotope analysis of ferric oxides, D. Schrag and D. Bryant for assistance in oxygen isotope analysis of water, and Rob Franks for measuring oxalate-extractable [Fe]. The paper benefited from careful reviews by J. R. O'Neil, Q. Williams, C. J. Yapp, and two anonymous reviewers. This research is supported by National Science Foundation grant EAR-9627953.

## REFERENCES

- Bao H., Koch P. L., and Rumble D III (in press) Paleocene/Eocene climatic variation in western North America: Evidence from the  $\delta^{18}\text{O}$  of pedogenic hematite. *GSA Bull.*
- Bao H. (1998) Ferric oxides and oxyhydroxides: Oxygen-isotope systematics and paleoclimatic reconstruction. Ph.D Dissertation, Princeton University.
- Becker R. H. and Clayton R. N. (1976) Oxygen isotope study of a Precambrian banded iron-formation, Hamersley Range, Western Australia. *Geochim. Cosmochim. Acta* **40**, 1153–1165.
- Bird M. I., Longstaffe F. J., Fyfe W. S., and Bildgen P. (1992) Oxygen-isotope systematics in a multiphase weathering system in Haiti. *Geochim. Cosmochim. Acta* **56**, 2831–2838.
- Bird M. I., Longstaffe F. J., and Fyfe W. S. (1993) Oxygen-isotope fractionation in titanium-oxide minerals at low temperature. *Geochim. Cosmochim. Acta* **57**, 3083–3091.
- Blattner P., Braithwaite W. R., and Glover R. B. (1983) New Evidence on magnetite oxygen isotope geothermometers at 175° and 112°C in Wairakei Steam pipelines (New Zealand). *Isot. Geosci.* **1**, 195–204.
- Chacko T., Hu X., Mayeda T. K., Clayton R. N., and Goldsmith J. R. (1996) Oxygen isotope fractionations in muscovite, phlogopite, and rutile. *Geochim. Cosmochim. Acta* **60**, 2595–2608.
- Clayton R. N. and Epstein S. (1958) The relationship between  $\text{O}^{18}/\text{O}^{16}$  ratios in coexisting quartz, carbonate, and iron oxides from various geological deposits. *J. Geol.* **66**, 352–373.
- Clayton R. N. and Epstein S. (1961) The use of oxygen isotopes in high-temperature geological thermometry. *J. Geol.* **69**, 447–452.
- Combes J. M., Manceau A., and Calas G. (1990) Formation of ferric oxides from aqueous solutions: A polyhedral approach by X-ray Absorption Spectroscopy: II. Hematite formation from ferric gels. *Geochim. Cosmochim. Acta* **54**, 1083–1091.
- Cornell R. M., Giovanoli R., and Schneider W. (1989) Review of hydrolysis of iron(III) and the crystallization of amorphous iron(III) hydroxide hydrate. *J. Chem. Tech. Biotechnol.* **46**, 115–134.
- Cornell R. M. and Schwertmann U. (1997) *The Iron Oxides*. VCH Publishers.
- Dousma J. and De Bruyn P. L. (1976) Hydrolysis-precipitation studies of iron solutions I. Model for hydrolysis and precipitation from Fe(III) nitrate solution. *J. Colloid Interface Sci.* **56**, 527–539.
- Drits V. A., Sakharov B. A., Salyn A. L., and Manceau A. (1993) Structural model for ferrihydrite. *Clay Mineral.* **28**, 185–207.
- Fischer W. R. and Schwertmann U. (1975) The formation of hematite from amorphous iron(III) hydroxide. *Clays Clay Mineral.* **23**, 33–37.
- Flynn C. M. Jr. (1984) Hydrolysis of inorganic iron(III) salts. *Chem. Rev.* **84**, 31–41.
- Friedman I. and O'Neil J. R. (1977) Compilation of stable isotope fractionation factors of geochemical interest. *USGS Prof. Paper* 440kk.
- Gamsjäger H. and Murmann R. K. (1983) Oxygen-18 exchange studies of aqua- and oxo-ions. In *Advances in Inorganic and Bioinorganic Mechanisms* (ed. A. G. Sykes), Vol. 2, pp. 317–380. Academic Press.
- Girard J.-P., Razanadranoroosa D., and Freyssinet P. (1997) Laser oxygen isotope analysis of weathering goethite from the lateritic profile of Yaou, French Guiana: paleoweathering and paleoclimatic implications. *Applied Geochemistry* **12**, 163–174.
- Grant M. and Jordan R. B. (1981) Kinetics of solvent water exchange on iron(III). *Inorg. Chem.* **20**, 55–60.
- Grundl T. and Delwiche J. (1993) Kinetics of ferric oxyhydroxide precipitation. *J. Contamin. Hydrol.* **14**, 71–97.
- James H. L. and Trendall A. F. (1982) Banded Iron Formation: Distribution in time and paleoenvironmental significance. In *Mineral Deposits and the Evolution of the Biosphere* (ed. H. D. Holland and M. Schidlowski), pp. 199–218. Springer-Verlag.
- Johnston J. H. and Lewis D. G. (1983) A detailed study of the transformation of ferrihydrite to hematite in an aqueous medium at 92°C. *Geochim. Cosmochim. Acta* **47**, 1823–1831.
- Landa E. R. and Gast R. G. (1973) Evaluation of crystallinity in hydrated ferric oxides. *Clays Clay Mineral.* **21**, 121–130.
- Lu G., McCabe C., Henry D. J., and Schedl A. (1994) Origin of hematite carrying a Late Paleozoic remagnetization in a quartz sandstone bed from the Silurian Rose Hill Formation, Virginia, USA. *Earth Planet. Sci. Lett.* **126**, 235–246.
- Manceau A. and Drits V. A. (1993) Local structure of ferrihydrite and ferroxylite by EXAFS spectroscopy. *Clay Mineral.* **29**, 165–184.
- Mckeague J. A. and Day J. H. (1966) Dithionite- and oxalate-extractable Fe and Al as aids in differentiating various classes of soils. *Can. J. Soil Sci.* **46**, 13–22.
- Melikhov I. V., Kozlovskaya L. B., Berliner L. B., and Prokofiev M. A. (1987) Kinetics of hydroxide Fe(III) solid phase formation. *J. Colloid Interface Sci.* **117**, 1–9.
- Müller J. (1995) Sauerstoff-Isotope von Eisenoxiden: Fraktionierung und Aussagen zum Paläoklima. *Sonderveröffentlichungen*, Geologisches Institut der Universität zu Köln; Köln, Nr. **104**, 88 p.
- Nahon D. B. (1986) Evolution of iron crusts in tropical landscapes. In *Rates of Chemical Weathering of Rocks and Minerals* (ed. S. M. Coleman and D. P. Dethier), pp. 169–191. Academic Press.
- O'Neil J. R. (1986) Theoretical and experimental aspects of isotopic fractionation. In *Stable Isotopes in High Temperature Geological Processes* (ed. J. W. Valley et al.), Vol. 16, pp. 1–40. *Rev. Mineral. Mineral. Soc. Amer.*
- Petránek J. and Van Houten F. B. (1997) Phanerozoic ooidal iron-stones. *Czech Geol. Surv. Special Papers* **7**, 71 p.

- Polyakov V. B. and Ustinov V. I. (1997) Isotope equilibrium constants ( $\beta^{18}\text{O}$ -factors) of corundum. *Geochem. Internat.* **35**, 897–903.
- Russell J. D. (1979) Infrared spectroscopy of ferrihydrite: Evidence for the presence of structural hydroxyl groups. *Clay Mineral.* **14**, 109–113.
- Savin S. M. and Lee M. (1988) Isotopic studies of phyllosilicates. In *Hydrous Phyllosilicates (Exclusive of Micas)*. Vol. 19, pp. 189–223. *Rev. Mineral.* **19**, Mineral. Soc. Amer.
- Schneider W. (1984) Hydrolysis of iron(III)—chaotic olation versus nucleation. *Comm. Inorgan. Chem.* **3**, 205–223.
- Schneider W. and Schwyn B. (1987) The hydrolysis of iron in synthetic biological and aquatic media. In *Aquatic Surface Chemistry* (ed. W. Stumm), pp. 167–194. Wiley.
- Schwertmann U. and Cornell R. M. (1991) *Iron Oxides in the Laboratory: Preparation and Characterization*. VCH Publishers.
- Schwertmann U. and Fischer W. R. (1973) Natural “amorphous” ferric hydroxide. *Geoderma* **10**, 237–247.
- Schwertmann U. and Murad E. (1983) Effect of pH on the formation of goethite and hematite from ferrihydrite. *Clays Clay Mineral.* **31**, 277–284.
- Sharp Z. D. and Kirschner D. L. (1994) Quartz-calcite oxygen isotope thermometry: A calibration based on natural isotopic variations. *Geochim. Cosmochim. Acta* **58**, 4491–4501.
- Singh B. and Gilkes R. J. (1991) Concentration of iron oxides from soil clays by 5 M NaOH treatment: The complete removal of sodalite and kaolin. *Clay Mineral.* **26**, 463–472.
- Stumm W. and Morgan J. (1981) *Aquatic Chemistry*. Wiley.
- Taylor H. P. Jr. (1968) The oxygen isotope geochemistry of igneous rocks. *Contrib. Mineral. Petrol.* **19**, 1–71.
- Tudge A. P. (1960) A method of analysis of oxygen isotopes in orthophosphate; its use in the measurement of paleotemperatures. *Geochim. Cosmochim. Acta* **18**, 81–93.
- Van der Woude J. H. A. and De Bruyn P. L. (1983) Formation of colloidal dispersions from supersaturated iron(III) nitrate solutions. I. Precipitation of amorphous iron hydroxides. *Colloid. Surfs.* **8**, 55–78.
- Van der Woude J. H. A. and De Bruyn P. L. (1984) Formation of colloidal dispersions from supersaturated iron(III) nitrate solutions. III. Development of goethite at room temperature. *Colloid. Surf.* **9**, 173–188.
- Van Houten F. B. (1973) Origin of Red Beds—A Review 1961–1972. *Ann. Rev. Earth Planet. Sci.* **1**, 39–61.
- von Gunten U. and Schneider W. (1991) Primary products of oxygenation of iron(II) at an oxic/anoxic boundary; nucleation, agglomeration and ageing. *J. Colloid Interface Sci.* **145**, 127–139.
- Walker T. R., Larson E. E., and Hoblitt R. P. (1981) Nature and origin of hematite in the Moenkopi Formation (Triassic), Colorado Plateau: A contribution to the origin of magnetism in red beds. *J. Geophys. Res.* **86**, 317–333.
- Walton A. G. (1967) *The Formation and Properties of Precipitates*. Interscience.
- Wendt H. (1973) Die Kinetik typischer Hydrolysereaktionen von mehrwertigen Kationen. *Chimia* **27**, 575–588.
- Yapp C. J. (1987) Oxygen and hydrogen isotope variations among goethites ( $\alpha$ -FeOOH) and the determination of paleotemperatures. *Geochim. Cosmochim. Acta* **51**, 355–364.
- Yapp C. J. (1990a) Oxygen isotopes in iron(III) oxides: 1, mineral-water fractionation factors. *Chem. Geol.* **85**, 329–335.
- Yapp C. J. (1990b) Oxygen isotopes in iron(III) oxides: 2, Possible constraints on the depositional environment of a Precambrian quartz-hematite banded iron formation. *Chem. Geol.* **85**, 337–344.
- Yapp C. J. (1991) Oxygen isotopes in an oolitic ironstone and the determination of goethite  $\delta^{18}\text{O}$  values by selective dissolution of impurities: The 5 M NaOH method. *Geochim. Cosmochim. Acta* **55**, 2627–2634.
- Yapp C. J. (1993a) The stable isotope geochemistry of low temperature Fe(III) and Al “oxides” with implications for continental paleoclimates. In *Climate Change in Continental Isotopic Records* (ed. P. K. Swart et al.), Vol. 78, pp. 285–294. Geophys. Monogr.
- Yapp C. J. (1993b) Paleoenvironmental and the oxygen isotope geochemistry of ironstone of the Upper Ordovician Neda Formation, Wisconsin, USA. *Geochim. Cosmochim. Acta* **57**, 2319–2327.
- Yapp C. J. (1997) An assessment of isotopic equilibrium of goethites from a bog iron deposits and a lateritic regolith. *Chem. Geol.* **135**, 159–171.
- Zhang Chuanlun et al. (1997) Physicochemical, mineralogical, and isotopic characterization of magnetite-rich iron oxides formed by thermophilic iron-reducing bacteria. *Geochim. Cosmochim. Acta* **61**, 4621–4632.
- Zheng Y-F (1991) Calculation of oxygen isotope fractionation in metal oxides. *Geochim. Cosmochim. Acta* **55**, 2299–2307.
- Zheng Y-F (1998) Oxygen isotope fractionation between hydroxide minerals and water. *Phys. Chem. Mineral.* **25**, 213–221.